Contract Number: IST-2000-28419

Technical Report HAR32TR-040922-DGMR20

Harmonoise WP 3 Engineering method for road traffic and railway noise after validation and fine-tuning

Type of document: Technical Report - Deliverable 18
Document identity: HAR32TR-040922-DGMR20
Date: 20 January 2005
Level of confidentiality: C

	Name	Date / Signature
Written by	Renez Nota, DGMR Robert Barelds, DGMR Dirk van Maercke, CSTB	
Agreed by	Hans van Leeuwen. DGMR	

Project funded by the EC under the Information Society and Technology (IST) Programme

Amendments

Version number	Amendment details	Date (dd.mm.yy)
00.01	Final draft 1	22.09.04
00.10	Final version	22.12.04
00.20	Final version including test cases	20.01.05

Approval by the WP3 Technical Committee

Organisation	Name	Date / Signature
AEA	Margreet Beuving	
CSTB	Dirk van Maercke	
CSTB	Jérôme Defrance	
DGMR	Hans van Leeuwen	
DGMR	Robert Barelds	
DGMR	Renez Nota	
SINTEF	Gunnar Taraldsen	
SNCF	Corinne Talotte	
SP	Hans Jonasson	
TRL	Greg Watts	

Distribution List

Organisation	Number of copies
SP	1
TRL	1
SNCF	1
CSTB	1
AEA	1
DGMR	1
SINTEF	1

SUMMARY

This report gives the description of the HARMONOISE engineering method after validation and fine-tuning. The Harmonoise WP 3 technical report HAR32TR-030715-DGMR10 (D17) gives the first description of the Engineering method for road traffic and railway noise. This first calculation method was available about a year ago. Based on report HAR32TR-030715-DGMR10 (D17) test software was built. This process was synchronous with the further development of the engineering method. The test software was used for validation purposes. Most of the engineering method validations are done in relation to the HARMONOISE reference method. It can be concluded that the method has been extensively validated through more than 15000 cases using this reference method. This reference method is based on scientific, theoretical techniques such as BEM and PE (Boundary Element Method. Meteo-BEM and Parabolic Equation). The complete HARMONOISE engineering method has been validated through a number of measurement sites also at larger distances up to 1200 m. The method has been fine-tuned for all the validation cases.

The propagation part is related to the point-to-point test software version V2.007, 7 October 2004. This version is used for the validation calculations for the WP 4 measurements. During and after these calculations there was the latest fine-tuning, which is the point-to-point test software version V2.008, 29 November 2004. These latest corrections are incorporated in this technical report.

The HARMONOISE engineering method has been developed for the calculation of the equivalent continuous A-weighted sound pressure levels caused by road traffic and railway noise under variable meteorological conditions. It contains a description of both railway and road traffic sources as well as a description of the attenuation during propagation.
The sound power output of individual, moving vehicles is combined into an equivalent sound power output for the total traffic flow, represented by a source line. Point-to-point propagation paths are obtained by segmentation of these source lines, resulting in mutually incoherent point sources with subsources at different heights.
The propagation method describes the attenuation between each point source and an arbitrary receiver point. The total, short-term noise level at the receiver point is determined by summation of all contributions from all point sources.
The computed short-term noise levels vary in time (e.g. by variations in traffic flow, meteorological propagation conditions). Long-term average noise levels such as L_{DEN} and L_{night} are obtained by combining of several representative short-term noise levels, weighted by their period of occurrence.

The engineering method is a flexible calculation method in such a way that it can be used both for detailed computations in case of noise assessment and for noise mapping. Especially for noise mapping the method can be used with limited data input since default values are provided.

The source model for road traffic noise is described in this report. The source data given, can be used for default values for road traffic noise. Additional new data can be used later on and also data for other (quiet and also noisier) road surfaces should be collected. For railway noise only the structure of the database is given in this report. For this noise source at this moment there is no default value. (Validation has been done with specifically measured source data).

The method calculates the short-term sound pressure level at certain receiver positions for different meteorological data. It requires wind speed, wind direction, temperature gradient and absolute temperature en humidity. This short-term sound pressure level at a certain receiver position is calculated by incoherent summation over a number of point-to-point contributions. The combination of all the short-term sound pressure levels at a certain receiver position with the duration of meteorological situations that occur during the day, evening en night period, gives the L_{den}.

This report also describes the method for the source segmentation. The chosen method is a method of projection on the source only. Since it was decided that the viewing angle for each source segment is relatively small and we are working with Fresnel zones the possible errors are very small and acceptable. This is also a compromise with calculation time.

Contributions from ground reflections and diffracting obstacles like barriers are determined by the use of Fresnel zones around the reflection points on terrain segments between source and receiver. This method has been extended to reflecting obstacles. The size of the zone depends on the wavelength of the sound. The model includes multiple screening by using the most efficient edges of each screen.

A concluding summary of the main advantages of HARMONOISE engineering method:

- Physical source model. The source model has different sources for different excitation techniques;
- It includes the latest road and railway noise source separation techniques;
- Modelling of different operating conditions (acceleration/deceleration, road surface, track corrections, wheel/track roughness);
- It has been validated through 5 years of measurements in 3 countries across Europe;
- Exists as engineering method supported by reference methods (not a point-to-point black box);
- 1/3-octave model;
- One propagation model for "all" sources: roads & railways;
- Fresnel zones for more continuous modelling of reflections from ground and objects;
- Full continuous model; no discontinuities due to geographic imperfections;
- Includes meteorological effects such as wind direction, wind speed and temperature gradients;
- Designed for noise mapping, impact assessments and detailed studies.

The HARMONOISE engineering method gives more accurate results than existing methods. The method is designed for noise mapping, impact assessments and detailed studies. All calculations can be done with the same calculation core. The accuracy and detail level of input data will determine the accuracy of all the calculated results.

Contents **PAGE**

1 INTRODUCTION

The HARMONOISE engineering method has been developed for the calculation of the equivalent continuous A-weighted sound pressure levels caused by road traffic and railway noise under variable meteorological conditions. It contains a description of both railway and road traffic sources as well as a description of the attenuation during propagation.

The sound power output of individual, moving vehicles is combined into an equivalent sound power output for the total traffic flow, represented by a source line. Point-to-point propagation paths are obtained by segmentation of these source lines, resulting in mutually incoherent point sources with subsources at different heights.
The propagation method describes the attenuation between each point source and an arbitrary receiver point. The total, short-term noise level at the receiver point is determined by summation of all contributions from all point sources.
The computed short-term noise levels vary in time (e.g. by variations in traffic flow, meteorological propagation conditions). Long-term average noise levels such as L_{DEN} and L_{night} are obtained by combining of several representative short-term noise levels, weighted by their period of occurrence.

The engineering method has been validated by numerous measurements [REF 12] and the propagation part is related to the point-to-point test software version V2.007, 7 October 2004. This version of the test software is used for the validation calculations for the WP 4 measurements. During and after these calculations there was the latest fine-tuning, which is the point-to-point test software version V2.008, 29 November 2004. These latest corrections are incorporated in this technical report.

2 SCOPE

The accuracy of the method and the limitations to its use are described in a separate report [REF 12]. In this report, calculated noise levels and emission values are compared with measured noise levels in a number of test maps. The method applies to the following levels of accuracy:

- 1 dB standard deviation for distances up to 100 m;
- 2 dB standard deviation for distances up to 2000 m in flat surroundings / behind 1st row of buildings;
- 5 dB standard deviation for distances up to 2000 m in hilly surroundings / behind 2nd row of buildings.

These requirements correspond with a 95% confidence interval of +/-2 dB, +/-4 dB and +/-10 dB respectively. The levels of accuracy apply to the shortest distance to a road or railway.

The engineering model is valid for the frequency range from 25 Hz to 10 kHz. It provides a computation by 1/3-octave bands at frequencies according to ISO-R-266.

2.1 Field of application

The engineering model serves multiple purposes. It can be used both for noise mapping and noise assessment or even more detailed calculations. For noise maps, large areas are under survey, whereas for assessment of noise limits, only one or a few roads and a block of houses or a small area will be the subject of the calculations. The latter need more accuracy than a large noise map. A follow up of a noise map is a survey with action plans. This result needs again more accuracy.

This raises the dilemma between accuracy and detail on the one hand and ease of use and simplicity on the other hand. It should be kept in mind that a model is just a model and will always be a simplified representation of the real world. The calculation must be as accurate as possible, but on the other hand it must be just as accurate as necessary because other factors (such as input parameters) might be much more inaccurate.

For the engineering model, the most ambitious aim was to calculate the short time Leq of one hour. This immission level is based on, for example, the average traffic flow during an hour, which does not mean the actual flow at the specific hour. The same applies to other parameters, especially to the meteorological data.

Three levels of application can be distinguished for the engineering model:

- Detailed calculations
- Assessment
- Noise mapping

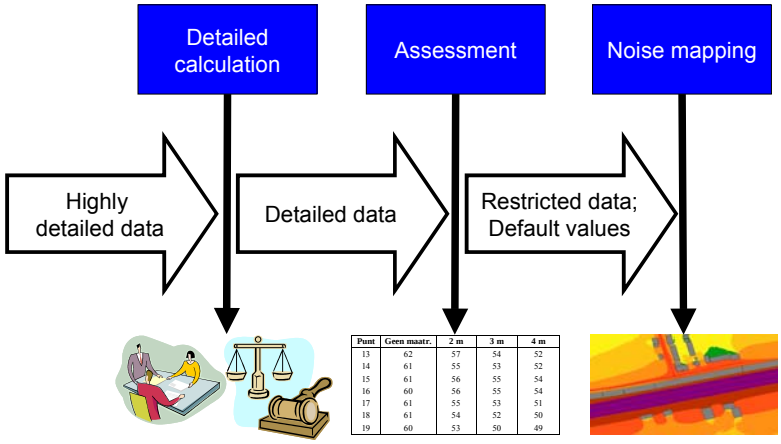

The most accurate application is used for detailed calculations. These calculations can be used for very critical situations, for example where there are a lot of discussions on noise levels perhaps even up to court. It is essential that the input data for these calculations is as accurate as possible. This might require detailed, measured input data such as ground impedances.
It has to be considered that for long-term average noise levels, annual and diurnal variations in the input data and the physical meaning and reality have to be taken into account.

For the assessment of situations such as the construction of new roads and railway lines or the development of new dwellings, it is necessary to calculate with detailed data but also with some default values.
Input data specific for the concerned project, such as traffic flow data and the geometry of the building plan, should be very detailed since such data are reasonably available.
Input parameters such as the meteorology and ground impedances will not always be obtainable, so default values from a global classification should be sufficient.

For noise mapping, it should be possible to use more general input for the necessary traffic data (standard vehicle distributions based on a road type classification) and the geometry should be less detailed in order to avoid time consuming calculations.

For this purpose, generalization of the geometry of roads/railways and buildings (that can be grouped into scattering zones) is recommended. Of course, this requires a clear guideline for such data reduction.

The accuracy of the noise calculations will depend on the accuracy of all input data. For calculations over large areas for noise mapping, the input data can be restricted to only the essential data. If no detailed data is available, default values should be provided. Due to the fact that the input information is limited the calculations are faster.
If there is more precise data, you can use it. For variant calculations, micro scale maps, for the study of individual localised problems, and to check legal limits of building levels you need more precise input data. We have to realise that data acquisition is a difficult part and possibly

the most expensive one. However it will be necessary to take care of the multiple use of this data. Data may be shared between different levels of use and serve different purposes.

The advantage of this approach is that only one engineering method has to be developed. There is no discrepancy between different models. For the development of more precise noise maps only the accuracy of input data is important. In the near future computation speed will increase so with a high detailed level of input data it will be possible to calculate in a limited time a large area. For the time being, precise input data can be generalised to rougher and only relevant data to speed up calculations. On the other hand, the user can use the principle from rough input data to more precise input data.

For noise mapping purposes, a single meteorological condition with three global meteorological corrections for the daytime, evening and night gives sufficient accuracy. This single meteorological condition must be representative for sound propagation with a positive, vertical sound speed gradient. The global meteorological corrections for each of the three periods is determined by the relative occurrence of such meteorological condition, irrespective of the direction of propagation, by the source and receiver height and by the source-receiver distance.

An enhancement of the computation of the noise levels is achieved by distinguishing the meteorological occurrence for each propagation path (wind direction) and combining sound propagation with a positive, vertical sound speed gradient with propagation in a homogeneous (neutral) atmosphere. This is obligatory for noise assessment. It may be assumed that meteorological conditions causing positive, vertical sound speed gradients and homogeneous conditions are complementary.

For a more detailed calculation, the number of meteorological conditions can be extended to a maximum number of 19, depending on the actual meteorological occurrences.

2.2 Frequency range

The engineering method is valid for the frequency range from 25 Hz to 10 kHz. It provides 1/3-octave band results at the frequencies displayed in table 2.1.

Based on these 1/3-octave band results, the A-weighted sound pressure level $L_{eq,1h}$ is computed by summation over all frequencies:

$$L_{eq1h} = 10 \lg \sum_{i=1}^{27} 10^{\left(L_{eq1h,i} + A_{f,i}\right)/10} \qquad (1)$$

where $A_{f,i}$ denotes the A-weighting correction according to IEC 651, given by table 2.1.

Table 2.1. Frequency range and A-weighting correction $A_{f,i}$

index (i)	freq [Hz]	$A_{f,i}$ [dB]	index (i)	freq [Hz]	$A_{f,i}$ [dB]	index (i)	freq [Hz]	$A_{f,I}$ [dB]
1	25	-44.7	10	200	-10.9	19	1600	+1.0
2	31.5	-39.4	11	250	-8.6	20	2000	+1.2
3	40	-34.6	12	315	-6.6	21	2500	+1.3
4	50	-30.2	13	400	-4.8	22	3150	+1.2
5	63	-26.2	14	500	-3.2	23	4000	+1.0
6	80	-22.5	15	630	-1.9	24	5000	+0.5
7	100	-19.1	16	800	-0.8	25	6300	-0.1
8	125	-16.1	17	1000	0.0	26	8000	-1.1
9	160	-13.4	18	1250	+0.6	27	10000	-2.5

3 DEFINITIONS

3.1 Conceptual definitions

Source line / source line segment

A source line is an approximate trajectory of a moving equivalent point source. For practical reasons, a source line can be approximated by a set of straight line segments (polyline), but it might as well be represented by a curve in space.

A source line has finite length, and it is represented by a set of incoherent point sources as the polyline is divided into source line segments. The definition of the source line segments depends on the propagation path detection method.

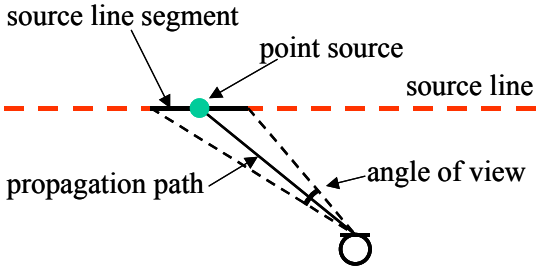

Fig. 1: Source line, source line segment, propagation path and angle of view

Propagation sector / angle of view

An angular sector drawn from the receiver to both ends of the source line segment. The angle between the lines from the receiver to both ends of the source line segment is called the *angle of view* of the propagation sector.

Propagation sectors may include reflections from nearly vertical obstacles by using the image of either the source or the receiver through the reflecting plane in place of the true position.

Homogeneous propagation sector

A propagation sector is considered to be homogeneous if the excess propagation attenuation within the sector is slowly varying with the position along the source line and if the excess attenuation can be calculated in a single representative propagation plane within the sector.

Point source

Source line segments will be represented by a number of mutually incoherent point sources at different height from which the acoustical energy radiates. Point source strength is expressed by the free-field acoustic source power level L_w per 1/1 or 1/3 octave band. All relevant parameters that define source strength will be incorporated, including horizontal and vertical directivity.

Point sources are situated at the intersections of each propagation path with each source line.

Vehicle model
The acoustical description of a single, moving vehicle at a specific speed and with specific driving conditions. A single vehicle might be composed of several mutually incoherent subsources at different positions, the strength of which is defined in terms of their sound power level.

Traffic model
The acoustical description of a traffic flow, based on the sound power levels of single moving vehicles. In the traffic model, the specific sound power output is combined with statistical data, yielding an equivalent noise emission for each subsource.

Receiver
A single point in which the acoustical energy will be calculated. A distinction should be made between free-field receivers that have propagation paths in all directions (360°) and receivers that represent the incoming acoustical energy for a façade. The latter will have a total viewing angle of 180° and a bisector perpendicular to the façade.

Propagation path / geometrical cross-section
The propagation path is the geometrical cross-section that represents the transmission path along which the acoustical energy from a single point source is transmitted towards a single receiver point. The propagation path is the bisector of a propagation sector.
Basically, it will be determined in a 2-dimensional way, in horizontal projection, starting from each receiver. However, the 2-dimensional cross-sections should be extended with a "2D½ geometrical analysis" in order to account for geometrical discontinuities in the vicinity of the propagation path.
A distinction can be made between propagation paths without a reflection and paths which include single or multiple reflections. The attenuation will be calculated along each propagation path.
The definition of the propagation path will be further dealt with in a specific technical report as a subtask of WP3.

Ray path
Each propagation path consists of a set of coherent ray paths. The shortest of these ray paths is called the "main ray path"; a ray path can be either direct (source in view of the receiver), reflected, diffracted or include any combination of these.
Ray paths are determined in a 3-dimensional way, in order to cope with complex geometries such as fly-overs, underpasses and roofings.

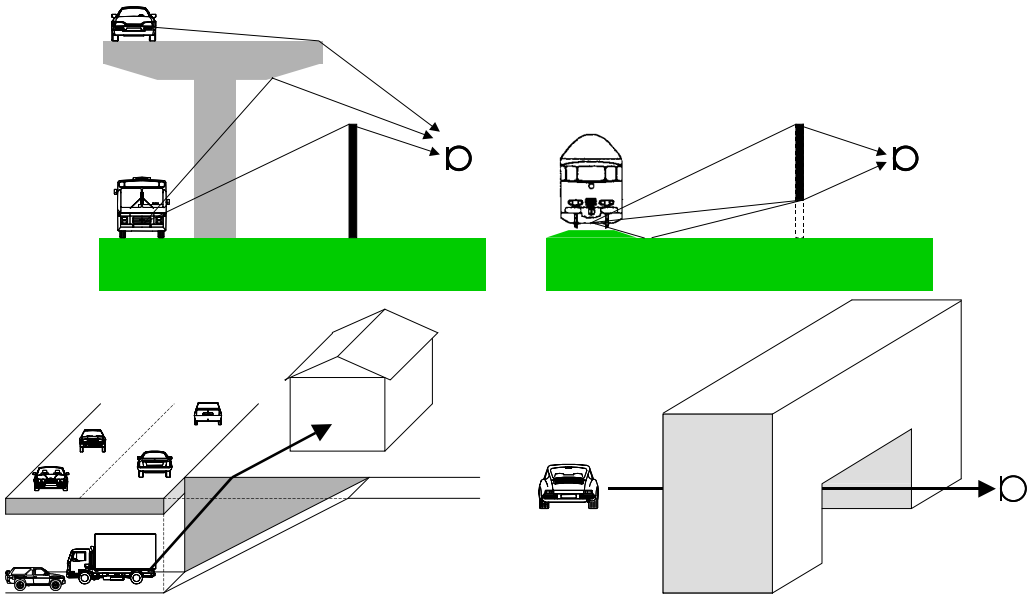

Fig. 2: Examples of ray paths in complex geometries

The two upper cases in Fig. 2 have additional ray paths compared with "regular" geometries. Advanced path detection methods are required in such cases. In the two lower cases it is more efficient to use algorithms for propagation through tunnels and for radiation from openings rather than generating numerous (higher order) reflection paths.

Wind speed and air temperature gradients cause vertical refraction of the ray path. For accurate calculation of propagation effects such as barrier attenuation and ground reflections, the definition of the ray path must comply with defined meteorological conditions that are representative for the site. Therefore, a distinction will be made between e.g. downwind propagation (downward refraction), propagation under neutral conditions (straight propagation paths) and eventually, upwind propagation (upward refraction). Positive temperature gradients have similar effects as downwind conditions.

Meteorological data

Since the definition of the propagation path depends on meteorological conditions, data on temperature gradients, wind speed and directions in relation to source and receiver must be collected. Furthermore, meteorological conditions such as temperature, snow covering and precipitation influence the sound power output of the sources. Such input data should be not too difficult to obtain, therefore associated parameters might be used, e.g. cloud covering for vertical temperature gradients.

Since momentary meteorological conditions, especially wind speed and direction, can vary rapidly, it is inevitable that a certain degree of classification is made. These meteorological classes must be defined such that variations within these classes have an acceptable effect on the predicted noise levels. At the same time, these meteorological classes must be realistic with regard to data collection and handling.

From each meteorological class, combined with possible variations in source strength, short term noise levels will be calculated. The yearly average noise indicators L_{den} and L_{night} can then be determined by the combination of these short term noise levels with their occurrence.
The meteorological classification will be subject to study in WP3, based on information from WP2.

Noise indicators
The long-term average noise indicator L_{DEN} is defined by:

$$L_{DEN} = 10 \lg\left[\frac{12}{24} * 10^{L_{eq,day}/10} + \frac{4}{24} * 10^{(L_{eq,evening}+5)/10} + \frac{8}{24} * 10^{(L_{eq,night}+10)/10}\right] \qquad (2)$$

where $L_{eq,\ day}$, $L_{eq,\ evening}$ and $L_{eq,\ night}$ are the yearly average equivalent sound pressure levels in the day, evening and night period respectively.

3.2 List of symbols

3.2.1 Indices

AN	aerodynamic noise
hor	horizontal
i	frequency index
m	vehicle category index
n	track type index
E	engine
R	receiver
RN	rolling noise
S	source
T	traction noise
vert	vertical

3.2.2 Geometrical and acoustical symbols

α	noise emission coefficient
α_{atm}	atmospheric attenuation coefficient
α_{road}	road gradient
a	acceleration
A_{atm}	attenuation due to atmospheric absorption
A_{diff}	attenuation due to diffraction by barriers
A_{div}	attenuation due to geometrical divergence
A_{excess}	excess attenuation
A_{gr}	attenuation due to ground effects
A_{refl}	attenuation due to energy loss during reflections
A_{scat}	attenuation due to scattering zones
β	noise emission speed coefficient
c	sound speed
C_{dc}	correction for driving conditions
C_{dir}	source directivity correction
C_{region}	regional correction for the vehicle fleet
C_{surf}	road surface correction (relative to the reference road surface and reference temperature)
δ	path length difference
f	frequency
F_{λ}	Fresnel coefficient
θ	angle of incidence (relative to the normal) / angle of diffraction
h	height relative to a ground segment
h_{eff}	effective height of a barrier
λ	wave length
L	source line segment length
L_w	sound power level
N	traffic flow

n_{axles}	number of axles for a heavy road vehicle
N_f	Fresnel number
p	sound pressure
Q	spherical reflection coefficient
R	point source-receiver distance by a straight line
ρ_E	energy reflection coefficient
R_{cur}	radius of curvature due to meteorological refraction
R_{hor}	horizontal projection of the point source-receiver distance
σ	flow resistivity
S	surface area
T_{atm}	air temperature
$T_{atm,0}$	reference air temperature
v	representative vehicle speed
v_{ref}	reference vehicle speed
w	Fresnel-zone weight
Z_0	specific acoustic impedance
z	height relative to a horizontal reference plane

4 SOURCE DESCRIPTION

4.1 General concept

In order to define the noise emission of a source line, two models are distinguished:

1. The vehicle model, describing the sound power of single moving vehicles;
2. The traffic model, combining the noise emission of numerous single vehicles into the sound power per metre length of the source line.

The vehicle model uses the vehicle speed as deterministic input data and yields the sound power output for a specific vehicle type. The traffic model gives a statistical description of sound power output of the total traffic flow.

4.2 Road traffic sources

4.2.1 Vehicle categorization

For road vehicles, 5 main classes (index m) are distinguished as presented in Tabel 4.1. This method provides noise emission parameters for main categories 1 through 3. For the assessment of the noise emission of vehicles in main categories 4 and 5 or for distinction of any subcategories, explicit measurement of the sound power levels is required. A description of the measurement method is given by [REF 1].

Table 4.1. Description of vehicle categorization

Main type	**m**	**Example of vehicle types**	**Notes**
Light vehicles	1a	Cars (incl MPV:s up to 7 seats)	2 axles, max 4 wheels
	1b	Vans, SUV, pickup trucks, RV, car+trailer or car+caravan(1), MPVs with 8-9 seats	2-4 axles*, max 2 wheels per axle
	1c	Electric vehicles	
	1d	Hybrid vehicles	
Medium heavy vehicles	2a	Buses	2 axles (6 wheels)
	2b	Light trucks and heavy vans	2 axles (6 wheels)(2)
	2c	Medium heavy trucks	2 axles (6 wheels)(2)
	2d	Trolley buses	2 axles (6 wheels)(2)
	2e	Low noise design	2 axles (6 wheels)(2)
Heavy vehicles	3a	Buses	3-4 axles
	3b	Heavy trucks	3 axles
	3c	Heavy trucks	4-5 axles
	3d	Heavy trucks	≥6 axles
	3e	Low noise design	≥3 axles
Other heavy vehicles	4a	Construction trucks (partly off-road use)	
	4b	Agr. tractors, machines, dumper trucks, tanks	
Two-wheelers	5a	Mopeds, scooters	Include also 3-wheel motorcycles
	5b	Motorcycles	

(1) 3-4 axles on car & trailer or car & caravan
(2) Also 4-wheel trucks, if it is evident that they are >3.5 tons

4.2.2 Source strength: main formula

The source power output by a separate moving vehicle is defined in terms of three subsources at 0.01m; 0.30m and 0.75m above the road surface. It is given for each vehicle category (m) and each 1/3 octave band (i) by equations 3 through 11.

<u>at 0.01m (m = 1,2,3):</u>

$$L_{W1,m,i} = L_{WRN1,m,i} \oplus L_{WTN1,m,i} \quad (3)$$

$$L_{WRN1,m,i} = \alpha_{RN,m,i} + \beta_{RN,m,i} \lg\left(\frac{v_m}{v_{ref,m}}\right) + 10\lg(0.8) + C_{dir,1,i} + C_{surf,m,i} + C_{region,m,i} \quad (4)$$

$$L_{WTN1,m,i} = \alpha_{T,m,i} + \beta_{T,m,i} \left(\frac{v_m - v_{ref,m}}{v_{ref,m}}\right) + 10\lg(0.2) + C_{dir,1,i} + C_{dc,m} \quad (5)$$

<u>at 0.30m (m = 1):</u>

$$L_{W2,m,i} = L_{WRN2,m,i} \oplus L_{WTN2,m,i} \quad (6)$$

$$L_{WRN2,m,i} = \alpha_{RN,m,i} + \beta_{RN,m,i} \lg\left(\frac{v_m}{v_{ref,m}}\right) + 10\lg(0.2) + C_{dir,2,i} + C_{surf,m,i} + C_{region,m,i} \quad (7)$$

$$L_{WTN2,m,i} = \alpha_{T,m,i} + \beta_{T,m,i} \left(\frac{v_m - v_{ref,m}}{v_{ref,m}}\right) + 10\lg(0.8) + C_{dir,2,i} + C_{dc,m} \quad (8)$$

<u>at 0.75m (m = 2,3):</u>

$$L_{W3,m,i} = L_{WRN3,m,i} \oplus L_{WTN3,m,i} \quad (9)$$

$$L_{WRN3,m,i} = \alpha_{RN,m,i} + \beta_{RN,m,i} \lg\left(\frac{v_m}{v_{ref,m}}\right) + 10\lg(0.2) + C_{dir,3,i} + C_{surf,m,i} + C_{region,m,i} \quad (10)$$

$$L_{WTN3,m,i} = \alpha_{T,m,i} + \beta_{T,m,i} \left(\frac{v_m - v_{ref,m}}{v_{ref,m}}\right) + 10\lg(0.8) + C_{dir,3,i} + C_{dc,m} \quad (11)$$

where

L_{WRN} is the rolling noise sound power;
L_{WTN} is the traction noise sound power;
α_{RN}, β_{RN} are rolling noise coefficients, given by table 4.2 [dB];
α_T, β_T are traction noise coefficients, given by table 4.3 [dB];
v is the vehicle speed [km/h];
v_{ref} is the reference vehicle speed [km/h];
C_{dc} is the correction for driving conditions [dB];
C_{dir} is the source directivity correction given in section 4.2.3 [dB];
C_{surf} is the road surface correction relative to a reference road surface [dB];
C_{region} is the correction for deviations in the sound power output of the regional vehicle fleet [dB].

The reference vehicle speed v_{ref} is 70 km/h, for all vehicle categories.

Table 4.2. Rolling noise coefficients

	Category 1		**Category 2**		**Category 3**	
freq [Hz]	**α_{RN}**	**β_{RN}**	**α_{RN}**	**β_{RN}**	**α_{RN}**	**β_{RN}**
25	69.9	33.0	76.5	33.0	80.5	33.0
31.5	69.9	33.0	76.5	33.0	80.5	33.0
40	69.9	33.0	76.5	33.0	80.5	33.0
50	74.9	15.2	78.5	30.0	82.5	30.0
63	74.9	15.2	79.5	30.0	83.5	30.0
80	74.9	15.2	79.5	30.0	83.5	30.0
100	77.3	41.0	82.5	41.0	86.5	41.0
125	77.5	41.2	84.3	41.2	88.3	41.2
160	78.1	42.3	84.7	42.3	88.7	42.3
200	78.3	41.8	84.3	41.8	88.3	41.8
250	78.9	38.6	87.4	38.6	91.4	38.6
315	77.8	35.5	88.2	35.5	92.2	35.5
400	78.5	31.7	92.0	31.7	96.0	31.7
500	81.9	21.5	94.1	21.5	98.1	21.5
630	84.1	21.2	93.8	21.2	97.8	21.2
800	86.5	23.5	94.4	23.5	98.4	23.5
1000	88.6	29.1	93.2	29.1	97.2	29.1
1250	88.2	33.5	90.6	33.5	94.6	33.5
1600	87.6	34.1	91.9	34.1	95.9	34.1
2000	85.8	35.1	86.5	35.1	90.5	35.1
2500	82.8	36.4	83.1	36.4	87.1	36.4
3150	80.2	37.4	81.1	37.4	85.1	37.4
4000	77.6	38.9	79.2	38.9	83.2	38.9
5000	75.0	39.7	77.3	39.7	81.3	39.7
6300	72.8	39.7	77.3	39.7	81.3	39.7
8000	70.4	39.7	77.3	39.7	81.3	39.7
10000	67.9	39.7	77.3	39.7	81.3	39.7

The noise emission coefficients α_{RN} for medium heavy vehicles (category 2) apply to 2 axles and heavy vehicles (category 3) apply to 5 axles. For vehicles with a different number of axles, the rolling noise sound power is found by using:

$$L_{WRN} = L_{WRN,2} + 10\lg\left(\frac{n_{axles}}{2}\right) \quad (12)$$

Table 4.3. Traction noise coefficients

	Category 1		Category 2		Category 3	
freq [Hz]	**α_T**	**β_T**	**α_T**	**β_T**	**α_T**	**β_T**
25	90.0	0.0	94.0	0.0	97.7	0.0
31.5	92.0	0.0	94.7	0.0	97.3	0.0
40	89.0	0.0	95.5	0.0	98.2	0.0
50	91.0	0.0	95.5	0.0	103.3	0.0
63	92.4	0.0	98.5	0.0	109.5	0.0
80	94.8	0.0	98.4	0.0	104.3	0.0
100	90.8	0.0	94.0	0.0	99.8	0.0
125	86.8	0.0	93.5	0.0	100.2	0.0
160	86.2	0.0	92.2	0.0	98.9	0.0
200	84.5	0.0	92.6	0.0	99.5	0.0
250	84.5	9.4	93.7	11.7	100.7	11.7
315	84.8	9.4	94.0	11.7	101.2	11.7
400	83.5	9.4	94.3	11.7	100.6	11.7
500	81.8	9.4	91.2	11.7	100.2	11.7
630	81.4	9.4	89.4	11.7	97.4	11.7
800	79.0	9.4	89.1	11.7	97.1	11.7
1000	79.2	9.4	90.8	11.7	97.8	11.7
1250	81.4	9.4	91.3	11.7	97.3	11.7
1600	85.5	9.4	92.2	11.7	95.8	11.7
2000	85.8	9.4	91.9	11.7	94.9	11.7
2500	85.2	9.4	90.3	11.7	92.7	11.7
3150	82.9	9.4	88.2	11.7	90.6	11.7
4000	81.0	9.4	86.3	11.7	89.9	11.7
5000	78.2	9.4	84.3	11.7	87.9	11.7
6300	77.2	9.4	82.3	11.7	85.9	11.7
8000	75.2	9.4	81.3	11.7	83.8	11.7
10000	74.2	9.4	80.3	11.7	82.2	11.7

The noise emission coefficients α and β apply to cruising vehicles on a dry reference road surface and at a reference road surface temperature. For deviations from these conditions, the corrections C_{dc} and C_{surf} are to be calculated. If specific data on the average sound power output of the local car fleet is available by measurement, this may be incorporated in terms of the regional correction C_{region}. Such a correction should be endorsed by measurements that meet the requirements in [REF 1]

4.2.3 *Horizontal and vertical directivity*

The directivity correction is composed of a horizontal and a vertical term. It is given by:

$$C_{dir,1,i} = C_{dir,hor,i} + C_{dir,vert,1,i} \quad \text{at 0.01m (m = 1,2,3)}$$
$$C_{dir,2,i} = C_{dir,vert,2,i} \quad \text{at 0.3m (m = 1)} \qquad (13)$$
$$C_{dir,3,i} = C_{dir,hor,i} + C_{dir,vert,3,i} \quad \text{at 0.75m (m = 2,3)}$$

where:

$$C_{dir,hor,i} = 0 \quad \text{for i = 1 to 18, 26 to 27} \qquad (14a)$$
$$C_{dir,hor,1,i} = \left(-1.5 + 2.5\left|\sin(\chi)\right|\right)\sqrt{\cos(\Psi)} \quad \text{for i = 19 to 25} \qquad (14b)$$
$$C_{dir,hor,3} = (1.546\ \chi^3 - 1.425\ \chi^2 + 0.22\ \chi + 0.6)\sqrt{\cos(\Psi)} \qquad (15)$$
$$\chi = \frac{\pi}{2} - \varphi \qquad (16)$$

where φ is the angle between the propagation path and the source segment in the horizontal plane in radians and Ψ is the vertical propagation angle (figure 3).

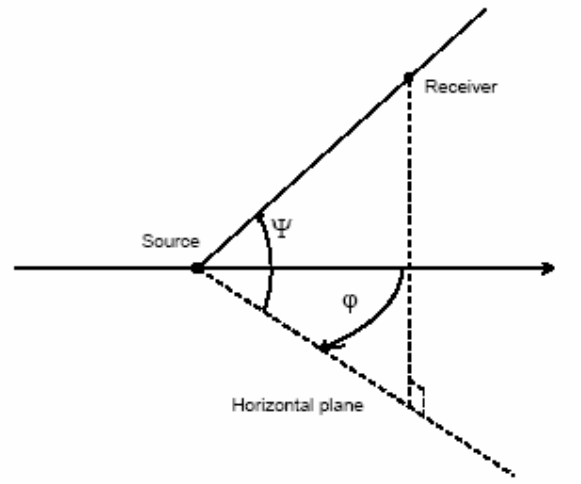

Fig. 3: Geometry for the horizontal and vertical directivity functions

The vertical directivity depends on frequency, source height and angle Ψ. It is given by equations 17a through 19c.

<u>at 0.01m:</u>

$$C_{dir,vert,1,i} = 0 \quad \text{for i = 1 to 9, 22 to 27} \qquad (17a)$$
$$C_{dir,vert,1,i} = -2\,(1-\cos^2(\Psi)) \quad \text{for i = 10 to 12} \qquad (17b)$$
$$C_{dir,vert,1,i} = -3\,(1-\cos^2(\Psi)) \quad \text{for i = 13 to 15} \qquad (17c)$$
$$C_{dir,vert,1,i} = -4\,(1-\cos^2(\Psi)) \quad \text{for i = 16 to 21} \qquad (17d)$$

at 0.30m:

$$C_{dir,vert,2,i} = 0 \quad \text{for i = 1 to 3} \quad (18a)$$

$$C_{dir,vert,2,i} = -2\sin(|\Psi|) \quad \text{for i = 4 to 6} \quad (18b)$$

$$C_{dir,vert,2,i} = -4\sin(|\Psi|) \quad \text{for i = 7 to 9} \quad (18c)$$

$$C_{dir,vert,2,i} = -5\,(1-\cos^2(\Psi)) \quad \text{for i = 10 to 15, 22 to 24} \quad (18d)$$

$$C_{dir,vert,2,i} = -6\,(1-\cos^2(\Psi)) \quad \text{for i = 16 to 21} \quad (18e)$$

$$C_{dir,vert,2,i} = -8\,(1-\cos(\Psi)) \quad \text{for i = 25 to 27} \quad (18f)$$

at 0.75m:

$$C_{dir,vert,3,i} = 0 \quad \text{for i = 1 to 9} \quad (19a)$$

$$C_{dir,vert,3,i} = -2\,(1-\cos^2(\Psi)) \quad \text{for i = 10 to 12, 19 to 27} \quad (19b)$$

$$C_{dir,vert,3,i} = -3\,(1-\cos^2(\Psi)) \quad \text{for i = 13 to 18} \quad (19c)$$

Note:
In case of diffraction by barriers or other obstacles, it should be taken into consideration that the vertical angle of propagation may differ strongly from the unobstructed case.

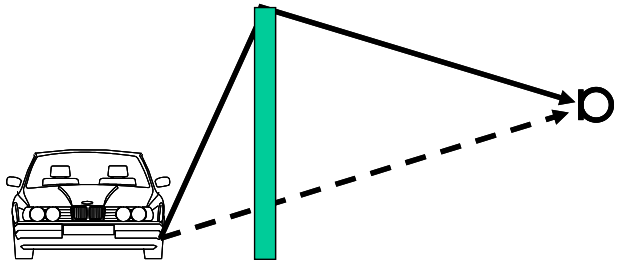

Fig. 4: Vertical angles of different ray paths in a diffraction case

4.2.4 *Road surface correction*

The noise emission parameters α,β apply to road vehicles on a reference surface. The following road surface types have been defined as reference road surfaces:

- Stone Mastic Asphalt (SMA): SMA 11-13, SMA 14-16
- Dense Asphalt Concrete (DAC): DAC 11-13, DAC 14-16

The numbers refer to the max. chipping size. 11-13 means that it could be any max. chipping size between 11 and 13 mm

For road surfaces other than a reference road surface at the reference temperature of 20 °C, the correction C_{surf} is to be applied. It is given by equation 20.

$$C_{surf,m,i} = \alpha_{surf,m,i} + \beta_{surf,m,i}\,\lg\left(\frac{v_m}{v_{ref,m}}\right) + K\left(T_{atm} - T_{atm,0}\right) \quad (20)$$

where:

α, β	are road surface coefficients [dB];
K	is the temperature coefficient [dB/°C]
T_{atm}	is the air temperature [°C];
$T_{atm,0}$	is the reference air temperature (=20 °C);

Road surface parameters α and β may be obtained from CPX measurement. Appendix A gives default values for some road surface types.

4.2.5 Correction for driving conditions and road gradients

No corrections are required for crossings without traffic lights. The calculations should be carried out like the case with an uninterrupted traffic flow.

For accelerating and decelerating vehicles, the correction for the driving conditions per vehicle category (m) is given by:

$$C_{dc,m} = C_m \; a_m \qquad \text{for } -2 \le a \le 2 \text{ m/s}^2 \qquad (21)$$

where:

a	is the acceleration/deceleration [m/s^2];
C	is the acceleration/deceleration coefficient [dBs^2/m], given by table 4.4.

Table 4.4. Acceleration/deceleration coefficient in dBs^2/m.

Main type	**C**
Light vehicles (m=1)	4.4
Medium heavy vehicles (m=2)	5.6
Heavy vehicles (m=3)	5.6

For medium heavy vehicles and heavy vehicles using their engine bakes on negative road gradients, the unsigned acceleration should be used.

For roads on a gradient, the change in engine noise will be taken into account in terms of a modified acceleration. It is given by:

$$a_m = a_{m,hor} + 10 \sin(\alpha_{road}) \qquad (22)$$

where α_{road} is the road gradient in radians. The correction to the traction noise is then given by equation 22.

4.3 Railway sources

The sound power output of railway sources is described by a database which contains source emission data on two levels:

- a parametrical model based on physical parameters, distinguishing subsources:
  - rolling noise
  - traction noise
  - aerodynamic and auxiliary sources
- sound power output for the whole vehicle based on a global description.

The parametrical model consist of two parts:

- A database file in MS-Access format;
- A source model "engine" which consists of the laws to obtain the output from the database;

The output of the emission data useful as input of the propagation calculation is:

- The sound power level (in third octave bands) of equivalent moving point sources for five possible heights as illustrated in figure 5.
- The associated directivity functions given in section 4.3.3

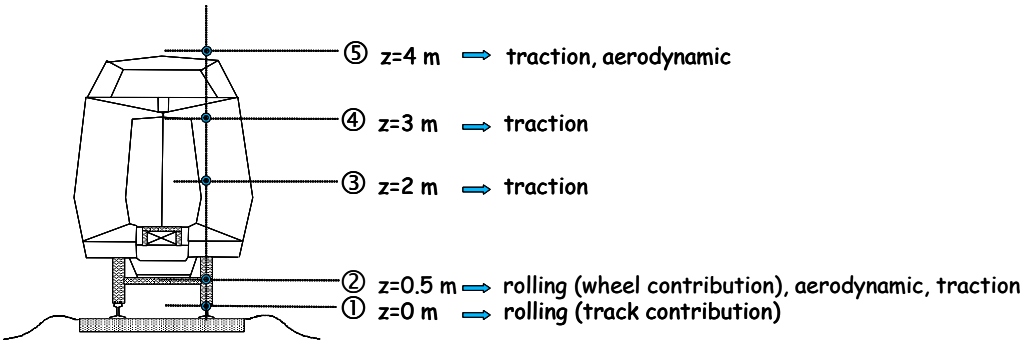

Fig. 5: Possible source heights for the railway source model

The sources which can be considered to be representative of railway emission are the rolling noise, the traction noise and the aerodynamic noise. Corrections to rolling noise are also proposed to describe special cases: impact, bridges, squeal and braking noise.

The following section gives a description of the source strength according to the detailed method. An escape is proposed to the user who has insufficient information to use the appropriate emission data for the partial sources and who can only get data provided by pass-by measurements for a whole vehicle or a train. In that case, the values of the sound power levels are directly implemented in the engineering model.

4.3.1 Track and vehicle categorization

The database is organised around two main tables which define the use of the other tables.

- One table which specifies the track characteristics, which are useful for the calculation of the rolling noise and the possible additional sources due to impact noise or bridge noise
- One table which specifies the vehicle characteristics. The vehicle categorization can be made according to the different partial sources that can describe it. We consider here vehicles concept which can be in practice vehicles or for some cases complete trains (like for EMUs, DMUs or High Speed Trains). We remind here that the database contents only examples for helping the understanding of the structure. The different countries are responsible of filling in the database following the practical methods proposed in HARMONOISE. An example of categorization is given hereafter in table 4.5.

Table 4.5. Example of vehicle categorization according to the type of source involved at the five possible source heights.

Vehicle type	**Source type at z=0 m**	**Source type at z=0.5 m**	**Source type at z=2 m**	**Source type at z=3 m**	**Source type at z=4 m**
Freight wagon	Rolling (track)	Rolling (wheel)	----	----	----
Passenger coach	Rolling (track)	Rolling (wheel)	Traction (drive)	----	----
Diesel locomotive	Rolling (track)	Rolling (wheel)	Traction (drive+fan +compressor)	----	Traction (exhaust)
Electric locomotive	Rolling (track)	Rolling (wheel)	Traction (drive+fan)	Traction (compressor)	----
DMU	Rolling (track)	Rolling (wheel)	Traction (drive+fan +compressor)	----	Traction (exhaust)
EMU	Rolling (track)	Rolling (wheel)	Traction (drive+fan)	Traction (compressor)	----
High speed train	Rolling (track)	Rolling (wheel) + aero bogie	----	----	Aero panto + traction (fan)

The other tables contain the data and the parameters useful to calculate the sound power according to the formulae given in the following section.

4.3.2 Source strength: main formula

The source power output by a separate moving vehicle is defined in terms of five subsources at 0.00m; 0.50m, 2m, 3m and 4m above the railhead. It is given for each vehicle category (m), track type (n) and each 1/3 octave band (i) by equations 23 through 33. Quantities defined in the wavelength domain (index j) are to be transformed to the frequency domain, using the relation λ = U/f.

at 0.00m (rolling noise):

$$L_{W1,m,n,i} = L_{r,total,m,n,i} + L_{Htr,n,i} + 10\lg(N_m) + C_{bridge,n,i} + C_{dir1} \quad (23)$$

$$L_{r,total,m,n,j} = L_{r,rail,n,j} \oplus L_{r,wheel,m,j} \oplus L_{r,impact,n,j} + CF_{m,n,j} \quad (24)$$

at 0.50m (rolling noise, traction noise, aerodynamic noise):

$$L_{W2,m,n,i} = \left[L_{WRN2,m,n,i} + 10\lg(N_m)\right] \oplus L_{WTN2,m,i} \oplus L_{WAN2,m,i} + C_{dir2} \quad (25)$$

$$L_{WRN2,m,n,i} = L_{r,total,m,n,i} + L_{Hveh,m,i} + C_{squeal,m,i} + C_{brake,m,i} \quad (26)$$

$$L_{WTN2,m,i} = L_{Wdrive2,m,ndrive\max,i} + C_{drive}\ \lg\left(\frac{n_{drive}}{n_{drive\max}}\right) \quad (27)$$

$$L_{WAN2,m,i} = L_{WANREF2,m,i} + \alpha_2\ \lg\left(\frac{U}{U_{ref2}}\right) \quad (28)$$

at 2m (traction noise):

$$\begin{aligned} L_{W3,m,i} = &\left[L_{Wfan3,m,n\max,i}\left(f\left(\frac{n_{fan\max}}{n_{fan}}\right)\right) + C_{fan}\ \lg\left(\frac{n_{fan}}{n_{fan\max}}\right) + 10\lg\left(dc_{fan}\right)\right] \\ &\oplus\left[L_{Wdrive3,m,ndrive\max,i}\left(f\left(\frac{n_{drive}}{n_{drive\max}}\right)\right) + C_{drive}\ \lg\left(\frac{n_{drive}}{n_{drive\max}}\right)\right] \\ &\oplus\left[L_{Wcomp3,m,i} + 10\lg\left(dc_{comp}\right)\right] + C_{dir3} \end{aligned} \quad (29)$$

at 3m (traction noise):

$$\begin{aligned} L_{W4,m,i} = &\left[L_{Wfan4,m,n\max,i}\left(f\left(\frac{n_{fan\max}}{n_{fan}}\right)\right) + C_{fan}\ \lg\left(\frac{n_{fan}}{n_{fan\max}}\right) + 10\lg\left(dc_{fan}\right)\right] \\ &\oplus\left[L_{Wdrive4,m,ndrive\max,i}\left(f\left(\frac{n_{drive}}{n_{drive\max}}\right)\right) + C_{drive}\ \lg\left(\frac{n_{drive}}{n_{drive\max}}\right)\right] \\ &\oplus\left[L_{Wcomp4,m,i} + 10\lg\left(dc_{comp}\right)\right] + C_{dir4} \end{aligned} \quad (30)$$

at 4m (traction noise, aerodynamic noise):

$$L_{W5,m,i} = L_{WTN5,m,i} \oplus L_{WAN5,m,i} + C_{dir5} \quad (31)$$

$$\begin{aligned} L_{WTN5,m,i} = &\left[L_{Wfan5,m,n\max,i}\left(f\left(\frac{n_{fan\max}}{n_{fan}}\right)\right) + C_{fan}\ \lg\left(\frac{n_{fan}}{n_{fan\max}}\right) + 10\lg\left(dc_{fan}\right)\right] \\ &\oplus\left[L_{Wexhaust5,m,i} + 10\lg\left(dc_{exhaust}\right)\right] \end{aligned} \quad (32)$$

$$L_{WAN5,m,i} = L_{WANREF5,m,i} + \alpha_5\ \lg\left(\frac{U}{U_{ref5}}\right) \quad (33)$$

where:

L_{WRN}	is the rolling noise sound power level [dB];
L_{WTN}	is the traction noise sound power level [dB];
L_{WAN}	is the aerodynamic noise sound power level [dB];
L_{WANREF}	is the aerodynamic noise sound power level at the reference speed [dB];
L_{Wdrive}	is the drive system sound power level [dB];
L_{Wfan}	is the fan noise sound power level [dB];
L_{Wcomp}	is the compressor sound power level [dB];
$L_{Wexhaust}$	is the exhaust sound power level [dB];
$L_{r,total}$	is the combined effective roughness frequency spectrum (wheel+rail+contact filter) at given speed [dB];
$L_{r,rail}$	is the rail roughness [dB];
$L_{r,wheel}$	is the wheel roughness [dB];
$L_{r,impact}$	is the effective equivalent roughness due to impact [dB];
CF	is the contact filter spectrum [dB];
L_{Htr}	is the transfer function from effective roughness to sound power for the track [dB];
L_{Hveh}	is the transfer function from effective roughness to sound power for the vehicle [dB];
N	is the number of axles per vehicle [-];
U	is the vehicle speed [km/h];
U_{ref}	is the reference speed for which L_{WAN} is given [km/h];
n_{fan}	is the fan rpm;
n_{fanmax}	is the maximum fan rpm;
n_{drive}	is the drive rpm;
$n_{drivemax}$	is the maximum drive rpm;
dc_{fan}	is the duty cycle for fans;
dc_{comp}	is the duty cycle for compressors;
C_{dir}	is the source directivity correction given in section 4.3.3 [dB];
C_{fan}	is the constant for rpm dependency of fan sound power;
C_{squeal}	is the correction for squeal noise [dB];
C_{brake}	is the correction for braking noise at given speed [dB];
C_{drive}	is a constant for rpm dependency of drive sound power [-];
α	is the speed coefficient for aerodynamic noise.

4.3.3 Directivity

For railway sources, only a horizontal directivity in considered. Three types of directivity functions can be chosen:

- A monopole directivity;
- A dipole directivity;
- A user-defined directivity, defined by 10°

The directivity function is given by:

$$C_{dir} = 0 \qquad \text{for monopole directivity} \qquad (34)$$

$$C_{dir} = 10 \lg\left(2 \cos^2 \chi\right) \qquad \text{for dipole directivity} \qquad (35)$$

$$\chi = \frac{\pi}{2} - \varphi \qquad (36)$$

where φ is the horizontal angle between the propagation path and the source segment in radians (figure 3).

4.4 Integration of sources

Based on the sound power output $L_{W,m,i}$ for a single moving vehicle (described in the sections 4.2 and 4.3), the average vehicle speed $\bar{v}_m$ and the traffic flow, the total sound power output of each subsource (at different source heights) of a source line with unit length is defined by equation 37.

$$L'_{W,m,i} = L_{W,m,i} + 10 \lg\left(\frac{Q_m \; v_0}{1000 \; Q_0 \; v_{eq,m}}\right) \qquad (37)$$

where

v_0 is the reference vehicle speed (1 km/h);
$v_{eq,m}$ is the equivalent vehicle speed for vehicle category m (km/h);
Q_0 is the reference traffic flow (1 h^{-1}).
Q_m is the traffic flow for vehicle category m (h^{-1}).

The total sound power output of a source line with unit length is obtained by summation over the different vehicle categories, given by equation 38.

$$L'_{W,i} = 10 \lg \sum_m 10^{0.1 \, L'_{W,m,i}} \qquad (38)$$

5 PROPAGATION PATHS: GENERAL CONCEPTS

The short-term, equivalent sound pressure level $L_{eq,1h,i}$ at a certain receiver position is calculated by incoherent summation over a number of point-to-point contributions from N propagation paths.

$$L_{eq1h,i} = 10 \lg \sum_{n=1}^{N} 10^{L_{eq1h,i,n}/10} \qquad (39)$$

The definition of point-to-point propagation paths is described in [REF 3]. For convenience, some general concepts are presented here.

5.1 Position of the sources

The vertical position of the sources has been described in sections 4.2 and 4.3. The lateral position of road traffic and railway sources is flush with the nearest wheel side. This requires a horizontal directivity function as illustrated in figure 6. The horizontal directivity function for road traffic noise is given in section 4.2.3.

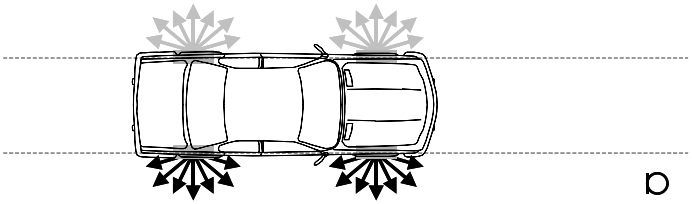

Fig. 6: Lateral position and horizontal directivity of the sources (receiver along the source line)

Receivers that are in line with the source segment require a different approach since both wheel sides contribute to these noise levels. This is illustrated in figure 7 below. If the receiver is between both (extended) source line segments of two wheel sides, the directivity of the sources is given by:

$$C_{dir,hor} = C_{dir,hor}(\varphi = 0) - 10 \lg(2) \qquad (40)$$

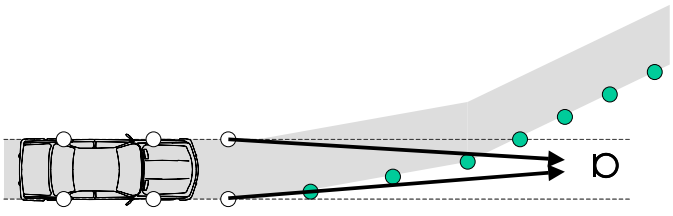

Fig. 7: Horizontal directivity of the sources (receiver in between extended source segments)

For convenience, the lateral position of the high railway sources (pantograph) is at the same lateral position as the other sources, i.e. at the railhead.

5.2 Source segmentation

The starting point for the source segmentation is a maximum viewing angle for each source segment as a general calculation parameter. For noise mapping purposes, a reasonable value for this maximum viewing angle is 5 degrees.

The relation between the viewing angle φ, propagation distance R and the 'optical' length of the source segment $\ell_{perspective}$ is given by equation 41:

$$\ell_{perspective} = 2\,R\,\tan(\phi/2) \qquad (41)$$

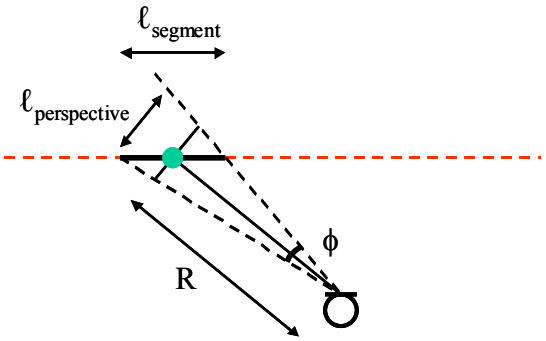

For propagation paths perpendicular to a straight source line, $\ell_{segment}$ equals $\ell_{perspective}$.

In the other extreme case, where the receiver is in line with a source line segment, the viewing angle equals zero. The source line segment length is then given by:

$$\ell_{segment} = \ell_{perspective} = 2\,R_{min}\,\tan(\phi_{max}/2) \qquad (42)$$

where φ_{max} is the general, maximum viewing angle and R_{min} is the propagation distance from the nearest point on the source line.

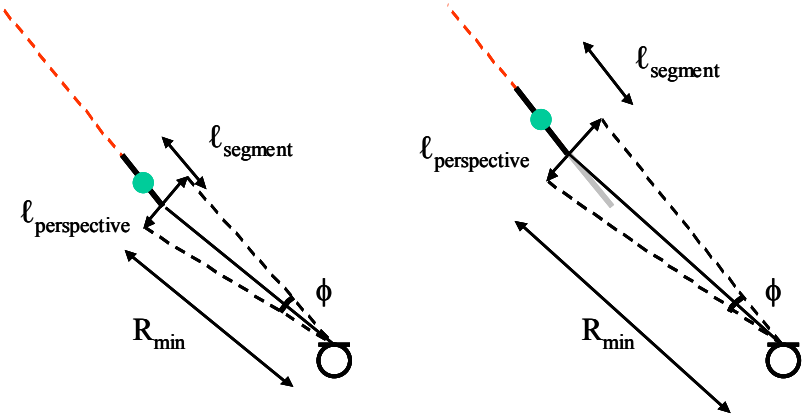

The starting point of the second source segment coincides with the end point of the first source segment, until the end of the source line is reached. The source point is situated halfway each source line segment.

More generally, the segmentation starts at the nearest point on the source line, irrespective of the position of vertices, working its way in two directions towards the end points of the source line.

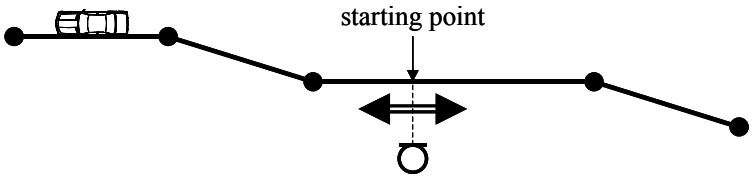

5.3 Propagation planes

Starting from a 3-dimensional geometry, consisting of source lines, buildings, ground planes and other objects such as embankments and noise barriers, a vertical propagation plane is constructed through each point source and each receiver point. In such a propagation plane, the geometry is reduced to two dimensions, however "out-of-the-plane"-corrections are included for reflections against finite-sized objects. The 2-dimensional geometry in the propagation plane is described in terms of ground segments.

5.4 Ray paths

Within each vertical propagation plane, different ray paths are distinguished, which can be mutually coherent. Figure 8 shows four ray paths for a case with diffraction by a barrier.

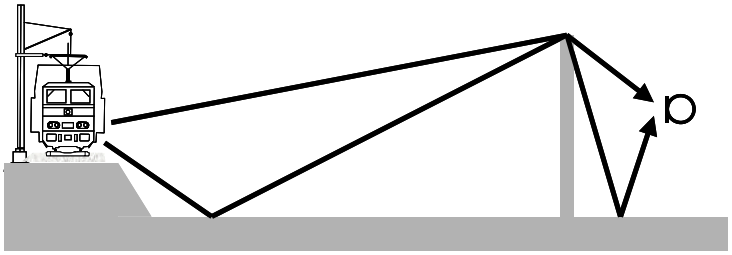

Fig. 8: Ray paths in a geometry with diffraction

5.5 Ground segments

Ground property and altitude variations are taken into account by representation of the terrain by ground segments. The total cross-section between the source and the receiver is formed by straight and homogeneous ground segments which have finite length (figure 9).

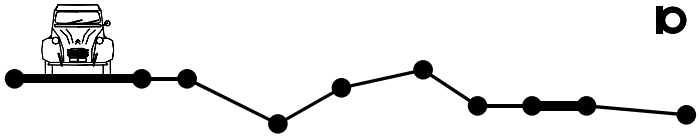

Fig. 9: Example of segmented terrain

An optional method for reducing the number of ground segments is provided by Appendix B.

5.6 Reflected propagation paths

Contributions from reflections are taken into account by the introduction of image sources or image receivers. For the generation of these reflected propagation paths, the initial sources that have been the result of the source segmentation as described in section 5.2, will be the starting point. Subsequent reflections are to be taken into account up to a maximum reflection depth of 3 reflections.
Tilted reflective planes may cause both vertically and horizontally reflected paths.

5.7 Fresnel-weighting

Contributions from different ground segments are combined by the use of Fresnel-zones around specular ray paths. The use is inspired by an approximate solution to predict sound propagation over flat terrain with varying surface types proposed by Hothersall and Harriott [hot1]. In this method the sound field at the receiver is assumed to be determined by the surface conditions in a region around the reflection point denoted the Fresnel-zone.
The Fresnel ellipsoid is defined by the locus of the points P defined by Equation 43 where S is the source point, R is the receiver point, and F_λ is a fraction of the wavelength λ. The foci of the ellipsoid are placed at S and R.

$$|SP| + |RP| - |SR| = F_\lambda \lambda \tag{43}$$

The Fresnel factor F_λ is equal to 1/16.
When the sound field is reflected by a flat surface, the elliptically shaped Fresnel-zone is defined by the intersection between the plane and the Fresnel ellipsoid with foci at the image source point S' and the receiver R as shown in figure 10.

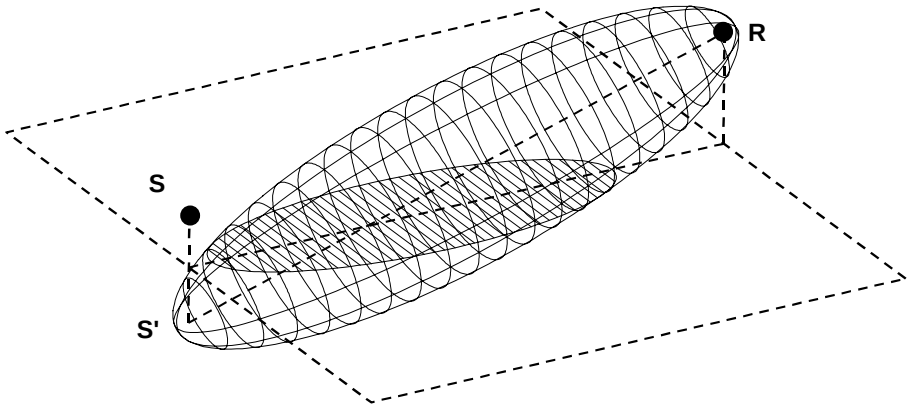

Fig. 10: Definition of Fresnel ellipsoid and Fresnel-zone

In a two-dimensional propagation model, the Fresnel-zone becomes one-dimensional as shown in figure 11.

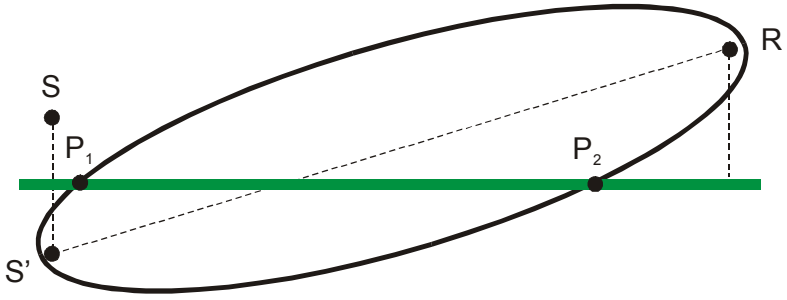

Fig. 11: One-dimensional Fresnel-zone (P1P2) in a two-dimensional propagation model

Algorithms for the calculation of the size of the Fresnel-zone are given in Appendix C.
The size of a sub-surface within the Fresnel-zone relative to the size of entire Fresnel-zone is used to determine the Fresnel-zone weight w_i which expresses the relative importance of the sub-surface. The Fresnel-zone weight is calculated according to Equation 44 where S_i is the area of the i'th sub-surface within the rectangular Fresnel-zone and S_{Fz} is the area of the entire Fresnel-zone as shown in figure 12.
In a two-dimensional propagation model, S_i and S_{Fz} are replaced by the lengths d_i and d_{Fz}.

$$w_i = \frac{S_i}{S_{Fz}} \approx \frac{d_i}{d_{Fz}} \tag{44}$$

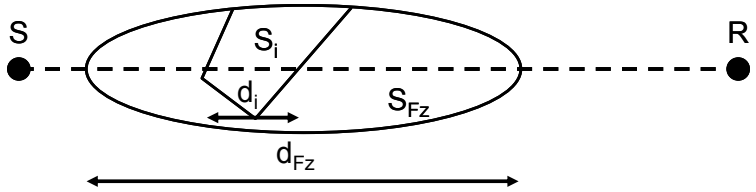

Fig. 12: Top view of a Fresnel-zone

5.8 Meteorological refraction

Vertical wind speed and air temperature gradients result in vertical sound speed gradients. These induce atmospheric refraction. This effect is taken into account by replacing the straight rays for a homogeneous atmosphere by curved rays. Based on its radius of curvature, each ray is fully described in terms of a height difference Δh relative to the straight ray.

$$\Delta h = \frac{R_{hor;S}\ R_{hor;R}}{2\ R_{cur}} \tag{45}$$

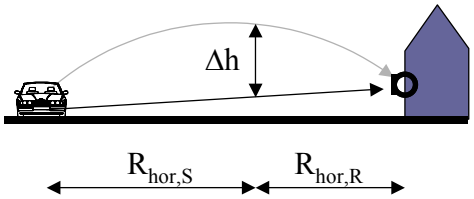

Fig. 13: Definition of curved rays

The radius of curvature R_{cur}, due to meteorological refraction, is given by:

$$\frac{1}{R_{cur}} = \frac{1}{R_A} + \frac{1}{R_B} \tag{46}$$

$$R_A = \frac{A}{|A|}\sqrt{\left(\frac{c_0}{|A|}\right)^2 + \left(\frac{D}{2}\right)^2} \tag{47}$$

$$R_B = \frac{B}{|B|}\frac{1}{8}\sqrt{\frac{2\pi c_0}{|B|}}D \tag{48}$$

where:

A is the linear sound speed coefficient in 1/s, given by equation 49a and 49b;
B is the logarithmic sound speed coefficient in m/s, given by equation 50
D is the horizontal distance between the source and the receiver in m;
c_0 is the reference sound speed = 331.4 m/s.

during day (stability classes S_1, S_2 and S_3:

$$A = \frac{u_*}{C_{vk}L} + \left(\frac{1}{2}\frac{c_0}{T_{ref}}\right)\left(0.74\frac{T_*}{C_{vk}L} - \frac{g}{c_p}\right) \tag{49a}$$

during night (stability classes S_4 and S_5:

$$A = 4.7\frac{u_*}{C_{vk}L} + \left(\frac{1}{2}\frac{c_0}{T_{ref}}\right)\left(4.7\frac{T_*}{C_{vk}L} - \frac{g}{c_p}\right) \tag{49b}$$

$$B = \frac{u_*}{C_{vk}} + \left(\frac{1}{2}\frac{c_0}{T_{ref}}\right)\left(0.74\frac{T_*}{C_{vk}}\right) \tag{50}$$

where:

u_* is the friction velocity in m/s, given by table5.3;
T_* is the temperature scale in K given by table 5.4;
L is the Monin-Obukhov length in m, 1/L given by table 5.5;
C_{vk} is the Von Karman constant = 0.4;
g is Newton's gravity acceleration = 9.81 m/s^2;
c_p is the the specific heat capacity of air at constant pressure, 1005 J/kg K;
T_{ref} is the reference temperature = 273 K.

The meteorological parameters u*, T* and the inverse of the Monin-Obukhov length, 1/L depend on the classification of the wind speed component in the direction of propagation and the atmospheric stability, given by tables 5.1 and 5.2 .

Table 5.1. Wind speed classification.

wind speed component at 10 m above ground	wind speed class
0 to 1 m/s	W1
1 to 3 m/s	W2
3 to 6 m/s	W3
6 to 10 m/s	W4
> 10 m/s	W5

Table 5.2. Classification of atmospheric stability.

time of day	cloud cover	stability class
day	0/8 to 2/8	S1
day	3/8 to 5/8	S2
day	6/8 to 8/8	S3
night	5/8 to 8/8	S4
night	0/8 to 4/8	S5

Table 5.3. Friction velocity, by wind speed class

wind speed class	u_* in m/s
W1	0.00
W2	0.13
W3	0.30
W4	0.53
W5	0.87

Table 5.4. Temperature scale T_*, by wind speed class and stability class

	S1	S2	S3	S4	S5
W1	-0.4	-0.2	0.0	+0.2	+0.4
W2	-0.2	-0.1	0.0	+0.1	+0.2
W3	-0.1	-0.05	0.0	+0.05	+0.1
W4	-0.05	0.0	0.0	0.0	+0.05
W5	0.0	0.0	0.0	0.0	0.0

Table 5.5. inverse of the Monin-Obukhov length 1/L, by wind speed class and stability class

	S1	S2	S3	S4	S5
W1	-0.08	-0.05	0.0	+0.04	+0.06
W2	-0.05	-0.02	0.0	+0.02	+0.04
W3	-0.02	-0.01	0.0	+0.01	+0.02
W4	-0.01	0.0	0.0	0.0	+0.01
W5	0.0	0.0	0.0	0.0	0.0

6 PROPAGATION: POINT-TO-POINT ATTENUATION

6.1 Main formula

The short-term, equivalent sound pressure level $L_{eq,1h,i,n}$ caused by a source segment n (represented by a point source with source power output L_W) is calculated by:

$$L_{eq1h,i,n} = L_{W,i} - A_{div} - A_{atm,i} - A_{excess,i} - A_{refl,i} - A_{scat,i} \quad (51)$$

where

$$L_{W,i} = L'_{W,i} + 10\lg(\ell_{segment}) \quad (52)$$

$L'_{W,i}$ is the sound power level of a unit length source segment, given by equation 38 in section 4.4 [dB];

$\ell_{segment}$ is the source segment length [m];

A_{div} is the attenuation due to geometrical spreading (section 6.2) [dB];

$A_{atm,i}$ is the attenuation due to atmospheric absorption (section 6.3) [dB];

$A_{excess,i}$ is the excess attenuation due to ground reflections and diffraction effects (section 6.4) [dB];

$A_{refl,i}$ is the attenuation due to energy loss during reflection (section 0) [dB];

$A_{scat,i}$ is the attenuation due to scattering zones (section 6.6) [dB].

6.2 Geometrical divergence

The geometrical divergence accounts for spherical spreading of the emitted acoustical energy from a point source in the free field. It does not depend on frequency and is given by:

$$A_{div} = 10\log\left[4\pi\left(\frac{R}{R_0}\right)^2\right] \quad (53)$$

where

R is the distance from the source to the receiver [m];

R_0 is the reference distance (1m).

6.3 Atmospheric absorption

The attenuation due to atmospheric absorption A_{atm} is given by:

$$A_{atm,i} = \alpha_{atm,i}\ R\ (1.0053255 - 0.00122622\ \alpha_{atm,i}\ R)^{1.6} \tag{54}$$

where

$\alpha_{atm,i}$ is the atmospheric attenuation coefficient in dB/m, given by [REF 4] for pure tones.

$$\alpha_{atm} = 8.686\ f^2 \left\{ \left[1.84 \times 10^{-11}\ \frac{p_r}{p_a} \sqrt{\frac{T}{T_0}} \right] + \left(\frac{T}{T_0} \right)^{-5/2} \left[\frac{0.01275\ \exp\left(\frac{-2\,239.1}{T} \right)}{f_{rO} + \left(\frac{f^2}{f_{rO}} \right)} + \frac{0.1068\ \exp\left(\frac{-3\,352.0}{T} \right)}{f_{rN} + \left(\frac{f^2}{f_{rN}} \right)} \right] \right\} \tag{55}$$

$$f_{rO} = \frac{p_a}{p_r} \left(24 + 4.04 \times 10^4\ h\ \frac{0.02 + h}{0.391 + h} \right) \tag{56}$$

$$f_{rN} = \frac{p_a}{p_r} \sqrt{\frac{T_0}{T}} \left(9 + 280\ h\ \exp\left\{ -4.170 \left[\left(\frac{T_0}{T} \right)^{1/3} - 1 \right] \right\} \right) \tag{57}$$

$$h = h_r\ \frac{p_r}{p_a}\ 10^C \tag{58}$$

$$C = -6.8346 \left(\frac{273.16}{T} \right)^{1.261} + 4.6151 \tag{59}$$

where

- T is the atmospheric temperature [K];
- T_0 is the reference temperature (= 293.15 K);
- h_r is the relative humidity [%];
- p_a is the atmospheric pressure [kPa];
- p_r is the reference atmospheric pressure (= 101.325 kPa).

6.4 Excess attenuation

In order to compute the total excess attenuation between a source segment and the receiver, a convex hull is to be constructed, starting from the source, over all ground segments towards the receiver. An example is given by figure 14.

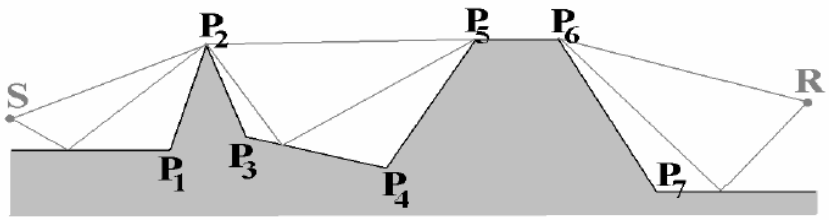

Fig. 14: Convex hull S-P_2-P_5-P_6-R between source and receiver points

After the convex hull has been constructed, the following steps are to be undertaken:

- Determine the insertion loss of all diffracting edges on the convex hull according to section 6.4.2;
- Calculate the ground effect between each set of two points on the convex hull.

The total excess attenuation between a source segment and the receiver is given by:

$$A_{excess,i} = \sum_{k=1}^{K} A_{diff,i,k} + \sum_{k=1}^{K+1} A_{gr,i,k} \qquad (60)$$

Where A_{diff} represents the attenuation due to diffraction for K points belonging to the convex hull and A_{gr} is the attenuation due to ground reflections for K+1 terrain sections in between two consecutive points on the convex hull.
The computation of A_{gr} is described in section 6.4.1, whereas the computation of A_{diff} is described in sections 6.4.2 and 6.4.3.

The method distinguishes three types of ground segments:

- concave ground segments;
- convex ground segments;
- ground segments that form a part of the convex hull.

For concave ground segments, the source and receiver are both above its extension to infinite length and the computation of Fresnel weights is straightforward as described in section 5.7.

A ground segment is considered convex if one of the source or the receiver (or either one of them replaced by the nearest diffracting edge on the convex hull) is below the extended segment. The Fresnel weight for convex ground segments is determined by a modified geometry, described in Appendix D.

A ground segment forms a part of the convex hull if both the source and the receiver and all of the (eventual) diffraction points are below its extension (the ground segment between P_5 and P_6 in fig 13). The attenuation by diffraction is computed as described in section 6.4.3. The ground attenuation for such segments is given in section 6.4.5.

6.4.1 *Flat ground model*

When sound propagates close to the ground, the direct sound interacts with the sound reflected from the ground. A simple approach to model this interaction when the terrain is flat with a homogeneous surface characterized by its specific acoustic impedance Z (section 6.4.6), is to represent the sound field by geometrical rays as shown in figure 15.

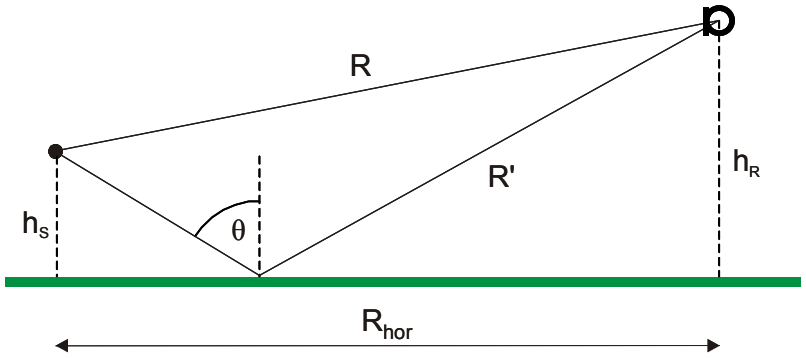

Fig. 15: Direct ray and ray reflected by the ground within a single propagation path

The ground attenuation is calculated according to equations 63 through 67 where R and R' are the path lengths of the direct and reflected ray, k is the wave number. Q is the spherical reflection coefficient as a function of the ground impedance Z, the reflection angle θ, and the distance R', according to Chien and Soroka [REF 5]. The calculation of Q is described in section 6.4.7. Path lengths R and R' are given by:

$$R = \sqrt{{R_{hor}}^2 + (h_S - h_R)^2} \tag{61}$$

$$R' = \sqrt{{R_{hor}}^2 + (h_S + h_R)^2} \tag{62}$$

Over flat terrain, the total ground attenuation A_{gr} is determined logarithmic weighting of the ground effects for the different ground segments N. For propagation over a terrain that can be described as a valley, linear Fresnel weighting is applied. Equation 63 gives a transition between both models based on the sum of the Fresnel weights.

$$A_{gr} = MIN\left[\chi_F \; A_{gr,flat} + (1-\chi_F)\; A_{gr,valley} \; ; 25\right] \tag{63}$$

where

$$\chi_F = \frac{1}{1+\left[MAX\left(\sum_{i=1}^{N} w_i \; ; 1\right) - 1\right]^2} \tag{64}$$

$$A_{gr,flat} = \sum_{i=1}^{N} w_i \; A_{gr,LOG,i} \tag{65}$$

$$A_{gr,LOG} = -10 \log\left(\left| 1 + C_{coh}\,\frac{R}{R'}\,Q\,e^{jk(R'-R)}\right|^2 + \left(1-{C_{coh}}^2\right)\left|\frac{R}{R'}\,Q\,e^{jk(R'-R)}\right|^2\right) \tag{66}$$

$$A_{gr,valley} = -10\log\left(\left|1+\sum_{i=1}^{N} w_i\, C_{coh}\,\frac{R}{R'}\,Q\,e^{jk(R'-R)}\right|^2 + \sum_{i=1}^{N} w_i\,\left(1-C_{coh}{}^2\right)\left|\frac{R}{R'}\,Q\,e^{jk(R'-R)}\right|^2\right) \quad (67)$$

and C_{coh} denotes the coherence loss factor given in section 6.3.

6.4.2 *Diffraction model*

For the insertion loss caused by a screening object, the solution of Deygout is applied. It is based on the Fresnel number N_f, given by equation 68:

$$N_f = sign(h_{eff})\frac{2(R_S + R_R - R)}{\lambda} \quad (68)$$

where

- h_{eff} is the effective height of the barrier;
- R_S is the path length between the source and the top edge of the barrier;
- R_R is the path length between the top edge of the barrier and the receiver;
- λ is the acoustic wavelength.

In Equation 68 sign(h_{eff}) is the signum function (sign = 1 for $h_{eff} > 0$, sign = 0 for $h_{eff} = 0$, sign = -1 for $h_{eff} < 0$).

An illustration of the geometrical quantities is given in figure 16.

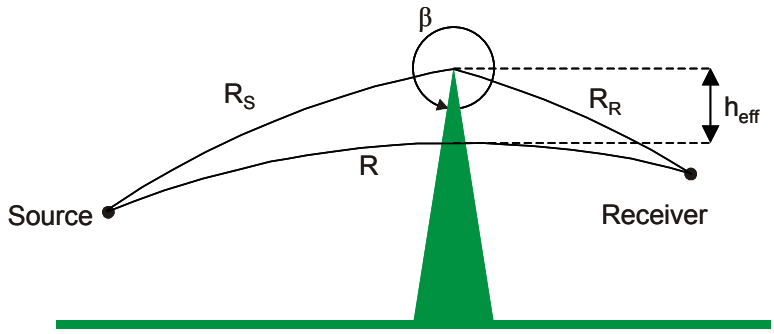

Fig. 16: Definition of quantities for diffraction over a sharp edge barrier

The attenuation due to diffraction by a barrier is given by:

$A_{diff} = 0$ for $N_f \le -0.25$ (69a)

$A_{diff} = 6 - 12\sqrt{-N_f}$ for $-0.25 \le N_f < 0$ (74b)

$A_{diff} = 6 + 12\sqrt{N_f}$ for $0 \le N_f < 0.25$ (74c)

$A_{diff} = 8 + 8\sqrt{N_f}$ for $0.25 \le N_f < 1$ (74d)

$A_{diff} = 16 + 10\lg N_f$ for $N_f \ge 1$ (74e)

6.4.3 *Multiple diffraction*

The solution for multiple diffractions is obtained by following the following procedure:

1. Determine the edge for which N_f has the maximum value in the absence of all other diffracting edges (most diffracting edge);
2. Determine the insertion loss A_{diff} (Equation 69) of this barrier alone using the true source and receiver position;
3. Depending on the position of the second barrier with respect to the first one, determine the insertion loss of the second barrier using the edge of the most diffracting barrier as the equivalent source or receiver position and sum the calculated insertion losses;
4. Repeat the previous step until all points on the convex hull have been found.

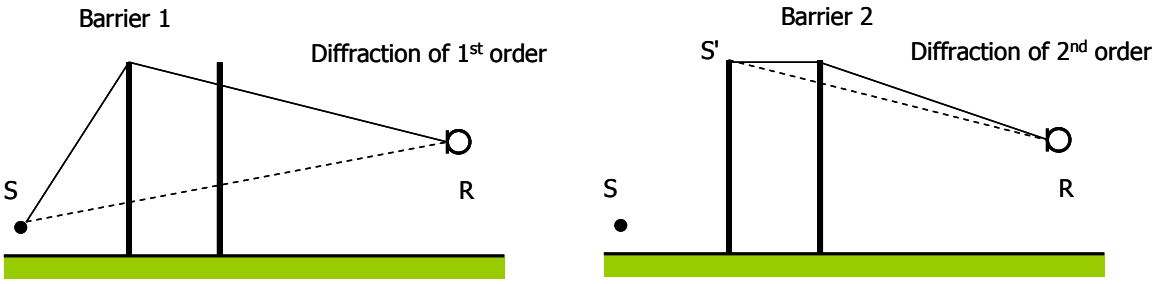

Fig. 17: Double diffraction

6.4.4 *Transition model*

If the ground profile between two points on the convex hull contains one or more convex segments, a transition is made between the flat ground model described in section 6.4.1 and the diffraction model. The diffracting point is the end point of a segment for which the (negative) path difference is closest to zero.

$$A_{gr} = \chi_T \; A_{trans,dif} + (1 - \chi_T) \; A_{trans,gr} \qquad (70)$$

$$A_{trans,dif} = A_{dif} + A_{gr,S} + A_{gr,R} \qquad (71)$$

$$\chi_T = \chi_3 + (1 - \chi_3) \; \chi_1 \; (1 - \chi_2) \qquad (72)$$

where $A_{trans,ground}$ denotes the ground effect between two points on the convex hull according to equation 70, A_{diff} denotes the diffraction effect described in section 6.4.2 and $A_{gr,S}$ and $A_{gr,R}$ are the ground attenuation on either side of the (secondary) diffracting point.

The transition parameter χ_1 is based on the path difference δ_{diff} and δ_{spec}. The path difference δ_{diff} is defined as the difference between the path through the diffracting point and the direct path. The path difference δ_{spec} is defined as the difference between the specularly reflected path and the direct path. This is illustrated in figure 18.
In the case that no specular reflection can be found, $\delta_{spec} = 0$ and in the case that more than one specular reflection occurs, the value of δ_{spec} closest to zero should be taken.

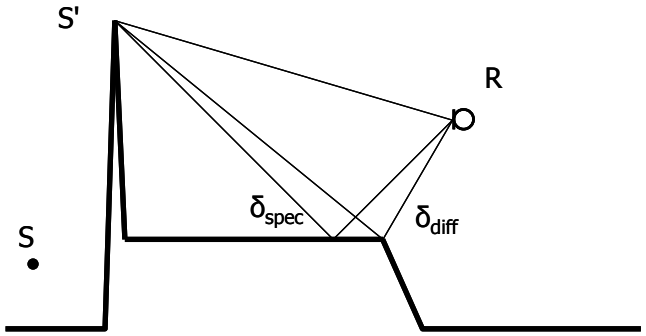

Fig. 18: Definition of path differences

Transition parameter χ_1 is given by:

$$\chi_1 = \exp\left(-\frac{\tau_1^{\,2}}{2}\right) \tag{73}$$

$$\tau_1 = \frac{\delta_{diff} - \delta_{spec}}{\lambda/4} \tag{74}$$

The transition parameters χ_2 is given by equations 75 through 77. In equation 77, the specular path differences of all segments (between the two points on the convex hull) are weighted, irrespective of the fact that the specular reflection point is on the segment or not.

$$\chi_2 = \exp\left(-\frac{\tau_2^{\,2}}{2}\right) \tag{75}$$

$$\tau_2 = \frac{\delta_{diff} - \overline{\delta_{spec}}}{\lambda/8} \tag{76}$$

$$\overline{\delta_{spec}} = \frac{\sum_k w_k \ \delta_{spec,k}}{\sum_k w_k} \tag{77}$$

Transition parameter χ_3 is given by:

$$\chi_3 = \exp\left(-\frac{\delta_{diff}}{\lambda/128}\right) \tag{78}$$

where λ is the sound wavelength in metres.

6.4.5 Thick barriers

In the case of a thick barrier, the convex hull coincides with one of the ground segments between two diffracting edges (P4 and P5 in figure 14). The ground effect for such a segment is computed as a transition between the logarithmically weighted ground effect $A_{gr,LOG}$ (equation 66) and the ground effect for a surface wave $A_{gr,surf}$:

$$A_{gr} = (1 - \alpha_{SW})\, A_{gr,LOG} + \alpha_{SW}\, A_{gr,surf} \quad (79)$$

with:

$$A_{gr,surf} = 6 + 0.3\left(A_{gr,LOG} - 6\right) \quad (80)$$

$$\alpha_{SW} = e^{-[MAX(h_S\,;\,h_R)/h_0]} \quad (81)$$

$$h_0 = \frac{2\,\pi\,c}{f\,|Z|} \quad (82)$$

where h_S and h_R are the source and receiver height relative to the ground segment, c is the speed of sound, f is the sound frequency and |Z| is the magnitude of the segment's ground impedance.

6.4.6 Ground impedance

The acoustic impedance Z of the ground can either be determined by direct measurement or by use of an impedance model. For non-porous ground surfaces, the acoustic impedance is given by the one-parameter model of Delany and Bazley [REF 6]:

$$Z = 1 + 9.08\left(\frac{f}{\sigma}\right)^{-0.75} + j\,11.9\left(\frac{f}{\sigma}\right)^{-0.73} \quad (83)$$

where f is the 1/3 octave band centre frequency in Hz and σ is the effective flow resistivity in $kNsm^{-4}$.

For convenience, default values for the effective flow resistivity σ are presented in table 6.1, based on a global description of the ground surface properties.

Table 6.1. Flow resistivity σ characterized by ground impedance classes

Description	**Representative flow resistivity σ ($kNsm^{-4}$)**
Very soft (snow or moss-like)	12.5
Soft forest floor (short, dense heather-like or thick moss)	31.5
Uncompacted, loose ground (turf, grass, loose soil)	80
Normal uncompacted ground (forest floors, pasture field)	200
Compacted field and gravel (compacted lawns, park area)	500
Compacted dense ground (gravel road, parking lot)	2000
Hard surface (dense asphalt, concrete, water)	200000

The impedance of a porous layer is determined by use of the impedance model by Hamet et al. [REF 7]. It is given by equations 84 through 89.

$$Z = \frac{q}{\Omega} F_{\mu}^{1/2} \left[\gamma - \frac{\gamma - 1}{F_{\theta}} \right]^{-1/2} \coth(-jkd) \quad (84)$$

where

$$k = \frac{q\,c}{2\,\pi\,f} F_{\mu}^{1/2} \left[\gamma - \frac{\gamma - 1}{F_{\theta}} \right]^{1/2} \quad (85)$$

$$F_{\mu} = \frac{1 + j\,f_{\mu}}{f} \quad (86)$$

$$F_{\theta} = \frac{1 + j\,f_{\theta}}{f} \quad (87)$$

$$f_{\mu} = \frac{\Omega\,\sigma}{2\,\pi\,\rho\,q^2} \quad (88)$$

$$f_{\theta} = \frac{\sigma}{2\,\pi\,\rho\,N_{pr}} \quad (89)$$

d is the layer thickness of the porous layer [m];
q^2 is the structure constant [-];
Ω is the layer porosity [-];
σ is the flow resistivity of the layer [$kNsm^{-4}$];
ρ is the density of air [kgm^{-3}];
c is the adiabatic sound speed [ms^{-1}];
f is the 1/3 octave band centre frequency y [Hz];
N_{pr} is the Prandtl number = 0.71 [-];
γ is the specific-heat ratio = 1.4 [-].

The density of air ρ and the adiabatic sound speed c are subject to atmospheric changes. By default, ρ = 1.225 kgm^{-3} and c =340.5 ms^{-1}.
For porous asphalt, the material parameters are given in the table below.

Table 6.2. Material parameters for porous asphalt

d [m]	**q^2 [-]**	**Ω [-]**	**σ [$kNsm^{-4}$]**
0.04	5	0.2	5

6.4.7 Spherical reflection coefficient

The spherical reflection coefficient Q is a function of the path length R' of the reflected ray, the reflection angle θ (equal to π/2 - ψ_G where ψ_G is the grazing angle), the wave number k and the normalised impedance Z. Q is calculated by equation 90 where $\Re_p(\theta)$ is the plane wave reflection coefficient calculated according to equation 91. The function $E(\rho_Z)$ is calculated by equations 92 and 93 where erfc(z) is the complementary error function extended to complex arguments.

$$Q = \Re_p(\theta) + \left(1 - \Re_p(\theta)\right) E(\rho_Z) \tag{90}$$

$$\Re_p(\theta) = \frac{\cos(\theta) - \frac{1}{Z}}{\cos(\theta) + \frac{1}{Z}} \tag{91}$$

$$E(\rho_Z) = 1 + j\sqrt{\pi}\,\rho_Z\, e^{-\rho^2} erfc\left(-j\rho_Z\right) \tag{92}$$

$$\rho_Z = \frac{1+j}{2}\sqrt{kR'}\left(\cos(\theta) + \frac{1}{Z}\right) \tag{93}$$

The complex function $w(\rho_Z) = \exp(-\rho_Z^2)\mathrm{erfc}(-j\rho_Z)$ in equation 92 can be determined by an approximate method as described in equation 94, which distinguishes three different domains for the real and imaginary parts x and y of $\rho_Z = x + jy$).

$x > 6 \vee y > 6$:

$$w(\rho_Z) = j\rho_Z\left(\frac{0.5124242}{\rho_Z^{\,2} - 0.2752551} + \frac{0.05176536}{\rho_Z^{\,2} - 2.724745}\right) \tag{94a}$$

$(3.9 < x < 6 \wedge y < 6) \vee (x < 6 \wedge 3 < y < 6)$:

$$w(\rho_Z) = j\rho_Z\left(\frac{0.4613135}{\rho_Z^{\,2} - 0.1901635} + \frac{0.09999216}{\rho_Z^{\,2} - 1.7844927} + \frac{0.002883894}{\rho_Z^{\,2} - 5.5253437}\right) \tag{94b}$$

$x < 3.9 \wedge y < 3$:

$$w(\rho_Z) = H + P_2 + j\left(K - Q_2\right) \tag{94c}$$

where

$$H = \frac{hy}{\pi\left(x^2 + y^2\right)} + \frac{2yh}{\pi}\sum_{n=1}^{5}\frac{e^{-n^2h^2}\left(x^2 + y^2 + n^2h^2\right)}{\left(y^2 - x^2 + n^2h^2\right)^2 + 4x^2y^2} \tag{95}$$

$$P_2 = 2e^{-\left(x^2 + 2y\pi/h - y^2\right)}\frac{A_1C_1 - B_1D_1}{C_1^2 + D_1^2} \tag{96}$$

$$K = \frac{hx}{\pi\left(x^2 + y^2\right)} + \frac{2xh}{\pi}\sum_{n=1}^{5}\frac{e^{-n^2h^2}\left(x^2 + y^2 - n^2h^2\right)}{\left(y^2 - x^2 + n^2h^2\right)^2 + 4x^2y^2} \tag{97}$$

$$Q_2 = 2e^{-\left(x^2 + 2y\pi/h - y^2\right)}\frac{A_1D_1 + B_1C_1}{C_1^2 + D_1^2} \tag{98}$$

$$h = 0.8 \tag{99}$$

$$A_1 = \cos(2xy) \tag{100}$$

$$B_1 = \sin(2xy) \tag{101}$$

$$C_1 = e^{-2y\pi/h} - \cos(2x\pi/h) \tag{102}$$

$$D_1 = \sin(2x\pi/h) \tag{103}$$

6.4.8 *Coherence loss*

The overall coherence factor C_{coh} denotes the loss of incoherency due to frequency band integration and due to turbulence.

$$C_{coh} = C_{fba}\ C_{turb} \tag{104}$$

The coherence factor due to frequency band averaging C_{fba} is given by:

$$C_{fba} = \frac{\sin\left[0.115\ k\ \left(R'-R\right)\right]}{0.115\ k\ \left(R'-R\right)} \qquad \text{for } 0.115\ k\ (R' - R) < \pi \tag{105A}$$

$$C_{fba} = 0 \qquad \text{for } 0.115\ k\ (R' - R) \geq \pi \tag{105B}$$

where k is the wave number and R' and R are defined according to equations 61 and 62.

The coherence factor due to turbulence C_{turb} is given by:

$$C_{turb} = \exp\left(-\frac{3}{8} 0.364\ F_k\ k^2 \gamma_\rho R\right) \tag{106}$$

$$\gamma_\rho = \left(\frac{h_S\ h_R}{h_S + h_R}\right)^{5/3} \tag{107}$$

where

- k is the wave number = $2\ \pi\ f\ /\ c$ [m^{-1}];
- R is the distance from the source to the receiver [m];
- F_k is Kolmogorov's structure parameter [$m^{2/3}s^{-1}$]
- h_S is the source height [m];
- h_R is the receiver height [m].

Typical values for the Kolmogorov structure parameter are between 10^{-7} and 10^{-5}.

6.5 Energy loss during reflection

The efficiency of the reflection is quantified by the reflection effect $A_{refl,i}$ calculated by equation 108. The first term in the equation is a correction for the effective energy reflection coefficient ρ_E and the second term is a correction for the size of the reflecting surface. $S_{refl,i}$ is the area of the surface within a Fresnel-zone in the plane of reflection and $S_{Fz,i}$ is the total area of the Fresnel-zone, which is determined by the intersection between the plane of reflection and the Fresnel ellipsoid around the sound ray from the image source to the receiver as shown in figure 10. The size of the Fresnel-zone is calculated based on a fraction $F_\lambda = 1/8$.
Any difference in directivity between the direct and reflected sound path is assumed to be incorporated in L_W in sections 4.2 and 4.3.

$$A_{refl,i} = 10\log\left(\rho_{E,i}\right) + 20\log\left(\frac{S_{refl,i}}{S_{Fz,i}}\right) \qquad (108)$$

Table 6.3 shows numeric examples for the broad-band energy reflection coefficient ρ_E.

Table 6.3. Examples for the broad-band energy reflection coefficient

Characteristics of reflecting surface	**ρ_E**
Plane and acoustically hard surface (concrete, stone, brick wall, metal sheets)	1.0
Non-absorbent building facades with windows and small irregularities, dense wooden panels	0.8
Factory walls with 50 % of the surface consisting of openings, installations or pipes	0.4

For a reflecting surface with a frequency dependent energy reflection coefficient, $\rho_{E,i}$ is calculated by equation 109 where α_i is the frequency dependent absorption coefficient.

$$\rho_E = 1 - \alpha \qquad (109)$$

If the surface is hard or almost hard with a rough texture of random nature, the reflection coefficient is estimated by equation 110 where k is the wave number, σ is the rms-value of the random (Gaussian) irregularities in the texture and θ is the angle of incidence (relative to the normal of the surface). σ can approximately be estimated by 0.3 times the peak to peak surface irregularities.

$$\rho_E = \exp\left(-2\left(k\,\sigma\cos\theta\right)^2\right) \qquad (110)$$

Irregularly shaped obstacles are to be divided into a number of sub-surfaces, each of which fulfils the requirement of being a plane surface, and the overall effect is obtained by a simple incoherent summation of the contributions from all surfaces.

6.6 Attenuation by scattering from trees

The attenuation as a result from propagation through (dense) forests is a function of the mean trunk diameter d, the total length of the sound path through the scattering zones R_{sc} and the average height of the trees h_{sc}. The length of R_{sc} is determined from the intersection of all scattering zones within the propagation path and the convex hull from the source to the receiver over all segments as illustrated below.

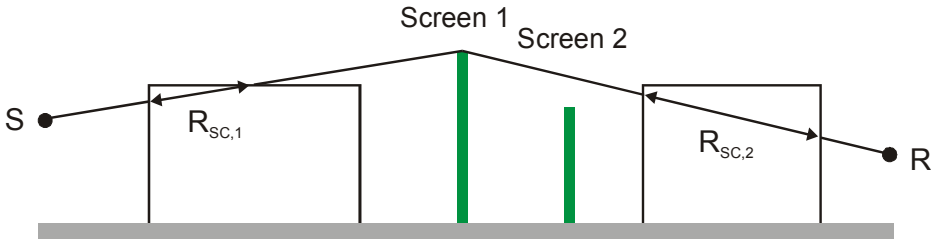

Fig. 19: Scattering zone path length R_{sc}

It is given by:

$$A_{scat,i} = MIN\left[1.25\, k_f(d)\left(\frac{R_{sc}}{43.75}\right)^2\left(A_e(h_{sc}, R_{sc}) + 20\lg\left(\frac{8\,R_{sc}}{25}\right)\right); 15\right] \qquad (111)$$

where the frequency weighting function $k_i(d)$ is given by table 6.4 and $A_e(h_{sc}, R_{sc})$ is given by table 6.5. The level correction A_e is to be determined by cubic interpolation from the scattering length R_{sc} and the average scattering height h_{sc}. If R_{sc} < 3.125 m, the effect of the scattering zone will be ignored.

Table 6.4. $k_f(d)$ as a function of wave number k and trunk diameter d in metres.

k d/2	≤ 0.7	1.0	1.5	3.0	5.0	10	≥ 20
k_i	0.00	0.05	0.20	0.70	0.82	0.95	1.00

Table 6.5. Level correction A_e as a function of R_{sc} and h_{sc}

R_{sc} [m]	**h_{sc} = 2.5 m**	**h_{sc} ≥ 25 m**
≤ 3.125	0.0	0.0
6.25	6.5	6.5
12.5	13.0	12.8
18.75	17.7	16.4
25	21.1	19.9
37.5	26.4	24.8
50	31.0	28.5
75	39.0	35.1
100	47.5	41.6
150	64.5	54.4
≥ 250	99.2	81.4

7 CONCLUSION

The engineering method is q flexible calculation method in such a way that it can be used both for detailed computations in case of noise assessment and for noise mapping. Esspecially for noise mapping the method can be used with limited data input since default values are provided.

The source model for road traffic noise is described in this report. The source data given, can be used for default values for road traffic noise. Future new available data can be used and also data for other (quiet and also noisier) road surfaces should be collected. For railway noise only the structure of the database is given in this report. For this noise source at this moment there is no default value. (Validation has been done with specifically measured source data).

The method calculates the short-term sound pressure level at certain receiver positions for different meteorological data. It requires wind speed, wind direction, temperature gradient and absolute temperature en humidity. This short-term sound pressure level at a certain receiver position is calculated by incoherent summation over a number of point-to-point contributions. The combination of all the short-term sound pressure level at a certain receiver position, with the duration of meteorological situations that occur during the day, evening en night period, gives the L_{den}.

This report also describes the method for the source segmentation. The chosen method is a method of projection on the source only. Since it was decided that the viewing angle for each source segment is relatively small and we are working with Fresnel zones the possible errors are very small and acceptable. This is also a compromise with calculation time.

Contributions from ground reflections and diffracting obstacles like barriers are determined by the use of Fresnel zones around the reflection points on terrain segments between source and receiver. This method has been extended to reflecting obstacles. The size of the zone depends on the wavelength of the sound. The model includes multiple screening by using the most efficient edges of each screen.

Generally it can be concluded that the Harmonoise Point to Pont method has been extensively validated on more than 15000 cases through the reference method which is based on scientific, theoretical techniques such as BEM and PE (Boundary Element Method. Meteo-BEM and Parabolic Equation). The complete HARMONOISE Engineering method has been validated to a number of measurement sites also at larger distances up to 1200 m. The method has been fine-tuned for all the validation cases.

A concluding summary of the main advantages of HARMONOISE engineering method:

- Physical source model. The source model has different sources for different excitation techniques;

- It includes the latest road and railway noise source separation techniques;
- Modelling of different operating conditions (accerlation/deceleration, road surface, track corrections, wheel/track roughness);
- It has been validated through 5 years of measurements in 3 countries across Europe;
- Exists as engineering method supported by reference methods (not a point-to-point black box);
- 1/3-octave model;
- One propagation model for "all" sources: roads & railways;
- Fresnel zones for more continuous modelling of reflections from ground and objects;
- Full continuous model; no discontinuities due to geographic imperfections;
- Includes meteorological effects as wind direction, wind speed and temperature gradients;
- Designed for noise mapping, impact assessments and detailed studies.

The HARMONOISE engineering method gives more accurate results than existing methods. The method is designed for noise mapping, impact assessments and detailed studies. All calculations can be done with the same calculation core. The accuracy and detail level of input data will determine the accuracy of all the calculated results.

8 RECOMMENDATION FOR FURTHER WORK

Further work on the propagation model has already started in the Imagine project, adding industrial & aircraft noise source models. Especially for industrial noise, lateral diffraction around vertical edges is relevant. Also data collection for the new source models is carried out.

For the propagation model there is a recommendation to carry out further research on the roughness (unevenness) of the surface. Terrain surface properties are characterized by the impedance and roughness of the surface. It will be necessary to study the effect of surface roughness more closely in the future.

The effect of wind on the sound speed profile has been discussed extensively in the technical meetings of WP 3. The solution is that we should introduce a displacement height for the sound speed profile. This displacement height must be dependent on the number and height of the buildings in a propagation cross section. A remark to this is that in urban situations the propagation distances are relatively short. Long propagation distances are related to highways and railway lines around an urban area. For these situations the existing method possibly over-estimates the ray curvature. On the other hand, RESWING effects may lead to underestimation of the sound speed gradient and hence the ray curvature. These principles have not been investigated.

The use of the method in the future and more validation of the method shall be done by all kind of different end users. These experiences and these validations may lead to adjustments of the method. It is recommended to establish a working group for maintenance of the source models, the source segmentation, the point to point method, the meteorological module. Errors and bugs can be corrected, versions will be reported and the software is public. It is recommended that no part of the engineering method is a "black-box". It is essential that every part of the engineering method can be checked by using the original formulas and algorithms.

9 REFERENCES

REF 1 HAR11TR-020301-SP02, "Determination of total sound power level of vehicles from pass-by measurements" (2002)

REF 2 HAR30TR-030106-DGMR01, "Harmonoise WP3, The engineering model: definitions" (2003)

REF 3 HAR31TR-030129-DGMR01, "Harmonoise WP3, Propagation paths and reflections" (2003)

REF 4 ISO 9613-1:1993(E), "Acoustics - Attenuation of sound during propagation outdoors- Part 1: Calculation of the absorption of sound by the atmosphere" (1993)

REF 5 C. F. Chien and W. W. Soroka: "A note on the calculation of sound propagation along an impedance boundary," J. Sound and Vibration. 69, 340-343 (1980)

REF 6 M. E. Delany and E. N. Bazley: "Acoustical properties of fibrous absorbant materials," Applied Acoustics. 3, 105-116 (1970)

REF 7 J.F. Hamet and M. Bérengier, "Acoustical characteristics of porous pavements: a new phenomenological model," Proc. Internoise 93 (Leuven, Belgium) 641-646 (1993).

REF 8 M.C. Bérengier, M.R. Stinson, G.A. Daigle, and J.F. Hamet, "Porous road pavements: Acoustical characterization and propagation effects," J. Acoust. Soc. Am. 101, 155-162 (1997)

REF 9 ISO 9613-2:1996(E), "Acoustics - Attenuation of sound during propagation outdoors- Part 2: General method of calculation" (1996)

REF 10 VDI 2714, "Schallausbreitung im Freien" (1988)

REF 11 B. Plovsing and J. Kragh, "Nord2000. Comprehensive Outdoor Sound Propagation Model. Part 1: Propagation in an Atmosphere without Significant Refraction," DELTA Acoustics & Vibration Report AV 1849/00, Lyngby (2001)

REF 12 HAR28TR-041109-TNO01, "Validation (D21) " (2004)

APPENDIX A: ROAD SURFACE CORRECTIONS

In addition to the road surfaces of the reference cluster the following road surface corrections $C_{surf,m,i}$, to be used in equations 4, 7 and 10, are available:

Table A.1. Road surface corrections for light vehicles (m=1)

	PAC[1] 6/16	2 layer PAC[1]	transversely brushed concrete	exposed aggregate concrete	SMA[2] 0/6	surface dressing 1/3	paving stones[3]	HRA 20[4]	block paving[5]
speed range	50-90	50-90	60-90	50-90	40-90	50-90	--	--	--
50 Hz		0.7		-3.3		0.8		0.0	
63 Hz		0.2		-3.1		-1.3		0.0	
80 Hz		3.6		-0.5		-0.4		0.0	
100 Hz	0.8	-1.0	-0.3	0.5	0.7	1.6	1.9	0.0	-5.4
125 Hz	1.3	-1.8	-0.8	0.0	-0.1	1.7	7.8	0.0	-1.1
160 Hz	1.3	-0.1	0.0	1.2	0.3	2.0	9.8	0.0	0.4
200 Hz	0.9	-0.9	0.7	0.7	-0.1	2.4	8.6	0.0	0.8
250 Hz	1.3	-0.7	2.2	1.7	0.6	2.8	9.1	0.0	2.3
315 Hz	2.5	-1.1	2.7	1.9	0.7	3.7	9.0	0.0	1.0
400 Hz	2.8	-0.5	3.4	2.2	0.9	4.3	8.4	0.0	-1.2
500 Hz	3.1	-1.5	3.0	2.8	1.7	5.0	11.3	2.2	0.9
630 Hz	2.8	-2.4	2.1	2.9	2.0	4.8	10.7	2.8	-0.9
800 Hz	-0.4	-3.0	2.0	2.9	0.2	4.4	9.2	4.2	0.1
1000 Hz	-3.0	-4.6	0.5	2.2	-1.9	4.1	7.8	5.3	1.5
1250 Hz	-4.2	-5.8	-0.1	1.7	-3.5	2.3	4.7	3.4	1.4
1600 Hz	-4.3	-6.5	1.0	0.7	-2.9	0.2	1.5	0.1	0.2
2000 Hz	-5.1	-7.9	1.7	-0.3	-3.0	-1.4	1.2	-1.4	-0.9
2500 Hz	-5.9	-7.8	1.4	-0.9	-2.5	-1.9	0.2	-2.8	-2.1
3150 Hz	-5.3	-7.2	0.1	-0.9	-2.5	-1.6	-0.2	-3.3	-2.6
4000 Hz	-3.7	-6.3	-0.5	-0.2	-1.8	-0.5	0.2	-4.1	-2.2
5000 Hz	-2.5	-5.6	-0.5	-0.5	-1.7	-0.3	0.1	-5.0	-1.7
6300 Hz	-2.1	-5.5	-1.3	-0.3	-6.0	-0.3	-0.6	-6.5	-2.7
8000 Hz	-1.0	-4.8	-1.8	-0.4	-6.0	0.0	-0.4	-6.9	-2.5
10000 Hz	-0.1	-4.3	-1.6	0.4	-4.8	0.3	-0.9	-8.5	-3.0

[1] PAC: Porous Asphalt Concrete

[2] SMA: Stone Mastic Asphalt

[3,5] see Fig. A.1

[4] HRA 20: hot rolled asphalt with 20 mm chippings rolled into the surface

Table A.2. Road surface corrections for medium heavy and heavy vehicles (m=2,3)

	PAC[1] 6/16	2 layer PAC[1]	transversely brushed concretey	exposed aggregate concrete	SMA[2] 0/6	surface dressing 1/3	paving stones[3]	HRA 20[4]
speed range	50-90	50-90	60-90	50-90	40-90	50-90	--	--
50 Hz		-1.8				-2.4		0.0
63 Hz		-3.4				-3.0		0.0
80 Hz		-1.5				-1.8		0.0
100 Hz	-0.2	-0.3	2.0	-0.4	0.9	0.9	4.5	0.0
125 Hz	-0.1	-1.5	2.8	0.4	1.6	1.1	6.7	0.0
160 Hz	0.3	-0.4	2.8	0.8	0.6	1.5	8.5	0.0
200 Hz	1.5	-0.5	3.5	1.6	1.7	2.1	3.7	0.0
250 Hz	2.0	-1.2	2.6	1.0	2.6	0.9	1.1	0.0
315 Hz	1.4	-1.1	1.9	0.3	1.1	1.1	1.2	0.0
400 Hz	-0.1	-3.3	3.2	1.1	1.3	2.0	5.9	0.0
500 Hz	0.0	-4.0	2.7	1.5	1.2	2.8	9.8	0.4
630 Hz	-4.4	-8.9	2.0	-0.4	-1.5	0.6	9.7	2.1
800 Hz	-5.9	-9.4	1.7	-0.5	-2.2	-0.9	6.5	2.2
1000 Hz	-5.9	-7.4	0.4	-1.4	-2.3	-2.1	3.1	1.4
1250 Hz	-5.1	-6.1	1.2	-1.4	-1.4	-2.1	1.7	1.1
1600 Hz	-3.1	-5.0	1.6	-0.3	0.3	-0.9	0.5	-0.5
2000 Hz	-2.0	-4.7	1.7	-0.3	1.0	-1.0	0.3	-1.7
2500 Hz	-5.1	-5.9	-0.1	-2.2	-0.9	-3.1	1.0	-1.4
3150 Hz	-4.9	-5.7	-1.1	-2.5	-1.1	-2.9	0.3	-2.3
4000 Hz	-1.7	-3.8	0.5	-0.7	1.7	-0.5	-0.9	-3.9
5000 Hz	-1.5	-3.6	0.1	-1.5	1.8	-1.0	0.2	-3.7
6300 Hz	-1.8	-4.0	0.2	-1.3	2.5	-0.6	-0.4	-5.2
8000 Hz	0.2	-2.7	0.6	-0.2	3.1	0.3	1.1	-5.3
10000 Hz	1.0	-2.9	0.5	-0.2	3.9	0.4	0.3	-7.4

[1] PAC: Porous Asphalt Concrete

[2] SMA: Stone Mastic Asphalt

[3] see Fig. A.1

[4] HRA 20: hot rolled asphalt with 20 mm chippings rolled into the surface

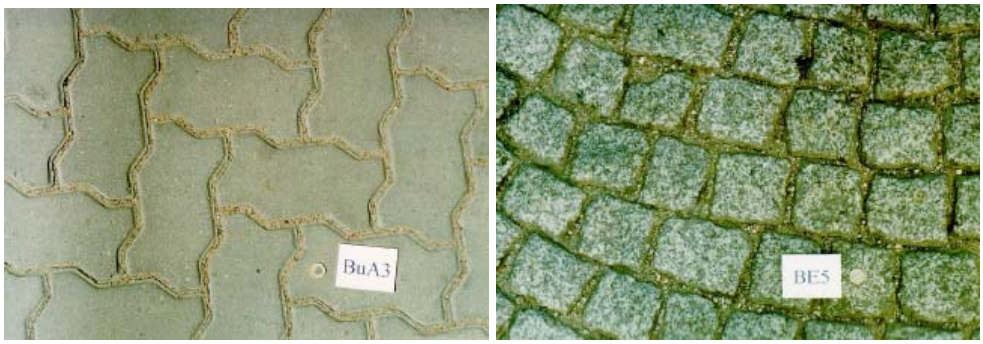

Fig. A.1 Example of block paving (left) and paving stones (right)

APPENDIX B: METHOD FOR OPTIMIZATION OF TERRAIN SEGMENTS (OPTIONAL)

Ground property and altitude variations are taken into account by representation of the terrain by ground segments. The total cross-section between the source and the receiver is formed by straight and homogeneous ground segments which have finite length (Fig. B.1).

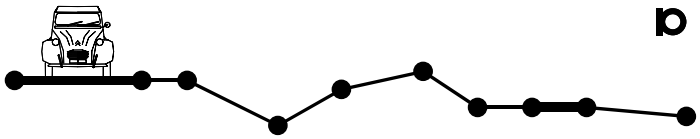

Fig. B.1 Example of segmented terrain

For the purpose of optimization, the number of ground segments may be reduced by grouping, based on "the maximum deviation principle". The ground point P having the maximum perpendicular distance r_{max} to the line between the first and the last ground point P_1 and P_2 will become a new ground point in the segmented terrain. The principle is illustrated in Fig. B.2.

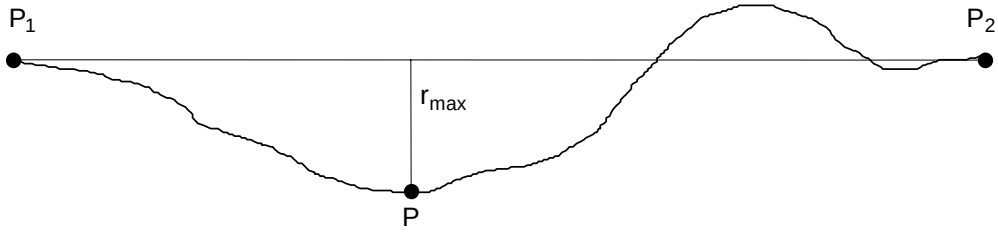

Fig. B.2: "Maximum deviation principle" used to determine a new ground point

Ground points between the source and the receiver are added successively to the segmented terrain until both of the following requirements are fulfilled:

- The maximum deviation r_{max} fulfils Eq. B.1
- The length of a segment d_{segm} fulfils Eq. B.2

$$r_{max} \leq \begin{cases} 0.1 & d \leq 50 \\ 0.002\,d & 50 < d < 500 \text{ (length in meters)} \\ 1 & d \geq 500 \end{cases} \quad \text{(B.1)}$$

$$d_{segm} \leq \begin{cases} 1 & d \leq 20 \\ 0.05\,d & 20 < d < 200 \text{ (length in meters)} \\ 10 & d \geq 200 \end{cases} \quad \text{(B.2)}$$

APPENDIX C: CALCULATION OF THE SIZE OF FRESNEL-ZONES

The point P on the Fresnel ellipsoid is defined by Eq. (C.1) where F_λ is the fraction of the wavelength λ.

$$|SP| + |PR| - |SR| = F_\lambda \lambda \quad \text{(C.1)}$$

The point O in Figure C.1 is the intersection between the source-receiver line SR and the Fresnel-zone plane, and $r_S = |SO|$ and $r_R = |RO|$

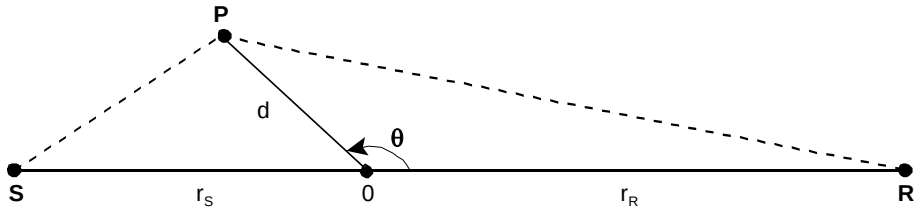

Fig. C.1 Geometrical definitions

The distance d = |OP| = f(r_S, r_R, θ) is calculated as shown below in Eqs. (C.2) through (C.7).

$$r = r_S + r_R \quad \text{(C.2)}$$

$$l = r + F_\lambda \lambda \quad \text{(C.3)}$$

$$A = 4\left(l^2 - (r\cos\theta)^2\right) \quad \text{(C.4)}$$

$$B = 4\, r\cos\theta\left(r_R^2 - r_S^2\right) + 4\left(r_S - r_R\right) l^2 \cos\theta \quad \text{(C.5)}$$

$$C = -l^4 + 2\left(r_S^2 + r_R^2\right) l^2 - \left(r_S^2 - r_R^2\right)^2 \quad \text{(C.6)}$$

$$d = \frac{-B + \sqrt{B^2 - 4AC}}{2A} \quad \text{(C.7)}$$

If $\theta = \pi/2$, $\cos\theta$ becomes 0 and the calculation of d can be simplified to Eq. (C.8).

$$d = \sqrt{\frac{\ell^2}{4} - \frac{r_S^2 + r_R^2}{2} + \frac{\left(r_S^2 - r_R^2\right)^2}{4\ell^2}} \quad \text{(C.8)}$$

If $\theta = \pi/2$ and $r_S = r_R$ the calculation of d can be further simplified to Eq. (C.9).

$$d = \sqrt{\frac{(F_\lambda \lambda)^2}{4} + \frac{F_\lambda \lambda}{2} r} \quad \text{(C.9)}$$

When source and receiver position relative to the reflecting ground surface are described by the source and receiver heights h_S and h_R and the horizontal distance d as shown in Figure C.2, the size of the Fresnel-zone is calculated as shown in the following. S' is the image source, R is the receiver and O is the reflection point.

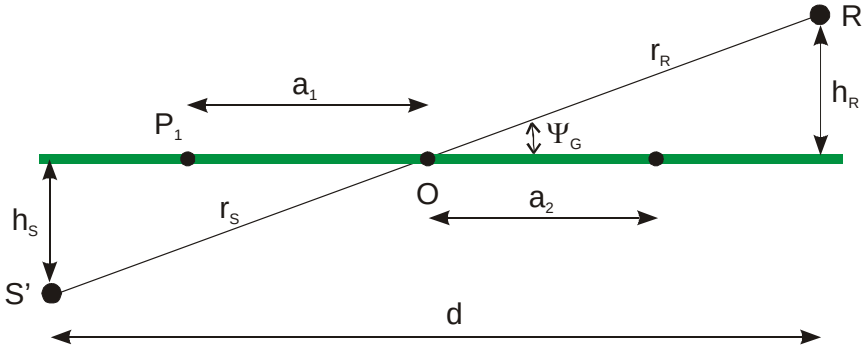

Fig. C.2 Geometrical definitions

$$\psi_G = \arctan\left(\frac{h_S + h_R}{d}\right) \tag{C.10}$$

$$r_{SR} = \sqrt{(h_S + h_R)^2 + d^2} \tag{C.11}$$

$$r_S = \frac{h_S}{h_S + h_R} r_{SR} \tag{C.12}$$

$$r_R = \frac{h_R}{h_S + h_R} r_{SR} \tag{C.13}$$

The size of the Fresnel-zone along the propagation path is $\left| P_1P_2 \right| = a_1 + a_2$ where a_1 and a_2 are calculated by Eqs. (C.14) and (C.15).

$$a_1 = \left| P_1O \right| = f\left(r_S, r_R, \pi - \psi_G\right) \tag{C.14}$$

$$a_2 = \left| P_2O \right| = f\left(r_S, r_R, \psi_G\right) \tag{C.15}$$

The size of the Fresnel-zone perpendicular to the propagation path is 2b where b is calculated by Eqs. (C.16) and (C.17). In this case the simple solution in Eq. (C.9) can be used to calculate b_0.

$$b_O = f\left(r_S, r_R, \frac{\pi}{2}\right) \tag{C.16}$$

$$b = \frac{b_O^2}{\sqrt{1 - \left(\frac{a_2 - a_1}{a_2 + a_1}\right)^2}} \tag{C.17}$$

APPENDIX D: CALCULATION OF FRESNEL ZONE WEIGHT

Fresnel weights are calculated in local coordinate systems attached to each segment. In the calculation procedures these coordinates are referred to as d (distance along the segment) and h (height relative to the segment).

The figure below shows the elementary geometry used in determination of the Fresnel weights in two dimensions. On input we are given:

- P_1 (x_1,y_1) : start point of the line segment
- P_2 (x_2,y_2) : end point of the line segment
- S (x_S,y_S) : position of the source ;
- R (x_R,y_R) : position of the receiver.

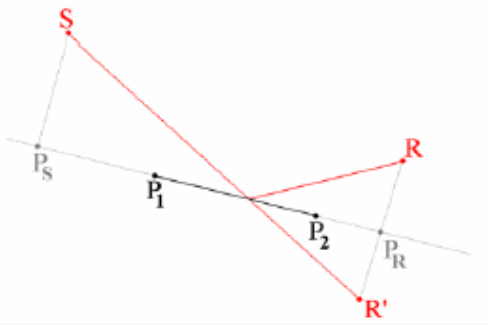

First we make a transform to a local coordinate system attached to the segment P_1-P_2. For this the local origin will coincide with P_1; the d-axis coincides with de segment and a normalized vector D(x_d,y_d) in this direction is given by:

$$x_d = \frac{(x_2 - x_1)}{d_{12}} \quad \text{(D.1)}$$

$$y_d = \frac{(y_2 - y_1)}{d_{12}} \quad \text{(D.2)}$$

$$d_{12} = \sqrt{(x_2 - x_1)^2 + (y_2 - y_1)^2} \quad \text{(D.3)}$$

The second normalized vector H (x_h,y_h) is chosen perpendicular to the first one:

$$x_h = -y_d \quad \text{(D.4)}$$

$$y_h = x_d \quad \text{(D.5)}$$

In this new coordinate system, the segment is now given by P_1 (0,0) and P_2 (d_{12},0) ; the source and receiver are given by S (d_S,h_S) and R (d_R,h_R) with:

$$d_S = (x_S - x_1)x_d + (y_S - y_1)y_d \quad \text{(D.6)}$$

$$h_S = (x_S - x_1)x_h + (y_S - y_1)y_h \quad \text{(D.7)}$$

$$d_R = (x_R - x_1)x_d + (y_R - y_1)y_d \quad \text{(D.8)}$$

$$h_R = (x_R - x_1)x_h + (y_R - y_1)y_h \quad \text{(D.9)}$$

All calculations can now be carried out in (d,h) coordinates.

Calculation of Fresnel weights for convex segments

A globally concave terrain may contain convex segments. In local coordinates, convex segments are identified by: $h_S < 0$ or $h_R < 0$. Note that it is not possible to have both $h_S < 0$ and $h_R < 0$ because this would imply that the segment is part of the convex hull.

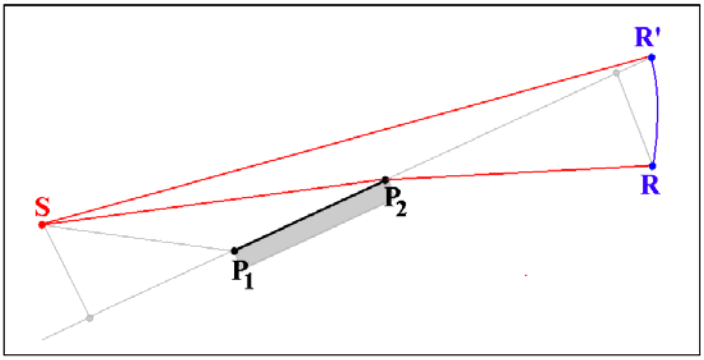

Fig. D.1 Geometrical definitions

In the case $h_R < 0$, the Fresnel weight of such segments is determined by (see fig D.1) :

- Replace R by R', the circular projection of R on the extended segment [P_1, P_2].
- Construct the Fresnel ellipse using S and R' instead of R.
- Calculate the Frensel weight *w'* of the segment [P_1, P_2] as usual.
- Determine *w* by :

$$w = w' \left| \frac{p_{dif}(S, P_2, R)}{p_{dif}(S, P_2, R')} \right|^2$$

Where $p_{dif}(S,P_2,R)$ and $p_{dif}(S,P_2,R')$ are calculated as if P_2 were a diffracting edge.

The case $h_S < 0$ is handled in a similar way.

If a convex segment occurs in between the source (or the receiver) and a diffracting edge or in between two diffracting edges, these edges will be used as equivalent source and/or receiver positions.

General rule :

"S" is the point on the convex hull left of and closest to P_1 ;

"R" is the point on the convex hull right of and closest to P_2.

APPENDIX E: Performance of the Harmonoise WP 3 Engineering method in urban situations - test cases

Contract Number: IST-2000-28419

Copy of
Technical Report HAR35TR-050111-DGMR10
Performance of the Harmonoise WP 3 Engineering method in urban situations - test cases

Type of document: Technical Report
Document identity: HAR35TR-050111-DGMR10
Date: 20 January 2005
Level of confidentiality: C

	Name	**Date / Signature**
Written by	Renez Nota, DGMR	
Agreed by	Hans van Leeuwen. DGMR	

Contents **PAGE**

1 INTRODUCTION

In [REF 1], a number of cases have been described where the performance and accuracy of both of the reference model and the engineering model should be tested. This memo gives a numerical description of 15 geometries that apply to these cases, and presents the results for different meteorological conditions.

2 CALCULATIONS

All computations have been carried out in line with the Harmonoise Engineering method described in [REF 2], using Predictor™ Type 7810 test software version X4.11. The propagation part is related to the Harmonoise point-to-point test software version V2.008, 29 November 2004.
Though the computations have been carried out by 1/3 octave bands, all results in this report are presented by 1/1-octave bands and after A-weighting correction according to IEC 651.

3 DESCRIPTION OF THE CASES

All items are defined in 3-dimensional ordinates, where the Z-ordinate is relative to a flat ground plane at Z=0.

Ground properties
Since all cases apply to an urban situation, the ground can be regarded as rigid (σ=20.000 kRayls) for the whole geometry.

Receivers
Two receiver types occur: a free-field receiver, subject to reflections from any building and a facade receiver (incident noise level), for which reflections from its facade are discarded. The number of the corresponding building is given in the field "Facade". All receivers are located at 4m above the ground.

Roads
Each geometry contains a double source line, consisting of three subsources at Z=0.01 m, 0.3 m and 0.75 m. The sound power level per metre length at the three different source heights is given by table 1 (for each source line). It corresponds with a traffic flow of 3000 light vehicles, 100 medium heavy vehicles and 50 heavy vehicles per hour, all cruising at 50 km/h of a reference road surface (DAC 0/11 - SMA 0/11) with an ambient temperature of 15 °C.

Table 1: (linear) sound power level per metre source length

	h_s = 0.01 m	h_s = 0.30 m	h_s = 0.75 m
25 Hz	69.0	72.62	71.1
32 Hz	70.2	74.42	71.4
40 Hz	70.5	74.32	72.2
50 Hz	71.6	74.34	74.5
63 Hz	79.0	83.42	79.7
80 Hz	78.8	84.02	76.9
100 Hz	73.6	78.33	72.5
125 Hz	71.0	73.63	72.5
160 Hz	70.4	73.69	71.2
200 Hz	71.0	71.83	74.5
250 Hz	69.9	70.58	73.3
315 Hz	70.2	70.59	73.7
400 Hz	70.1	70.57	71.3
500 Hz	72.3	67.51	68.7
630 Hz	73.5	68.34	68.3
800 Hz	74.2	68.30	66.3
1000 Hz	74.3	68.79	66.6
1250 Hz	73.1	69.10	66.3
1600 Hz	72.6	69.28	66.4
2000 Hz	70.9	68.73	66.1
2500 Hz	68.9	67.32	64.6
3150 Hz	66.2	65.99	62.8
4000 Hz	63.6	63.90	61.3
5000 Hz	61.1	61.96	59.0
6300 Hz	59.5	60.84	57.8
8000 Hz	57.3	58.80	55.2
10000 Hz	55.3	56.74	54.1

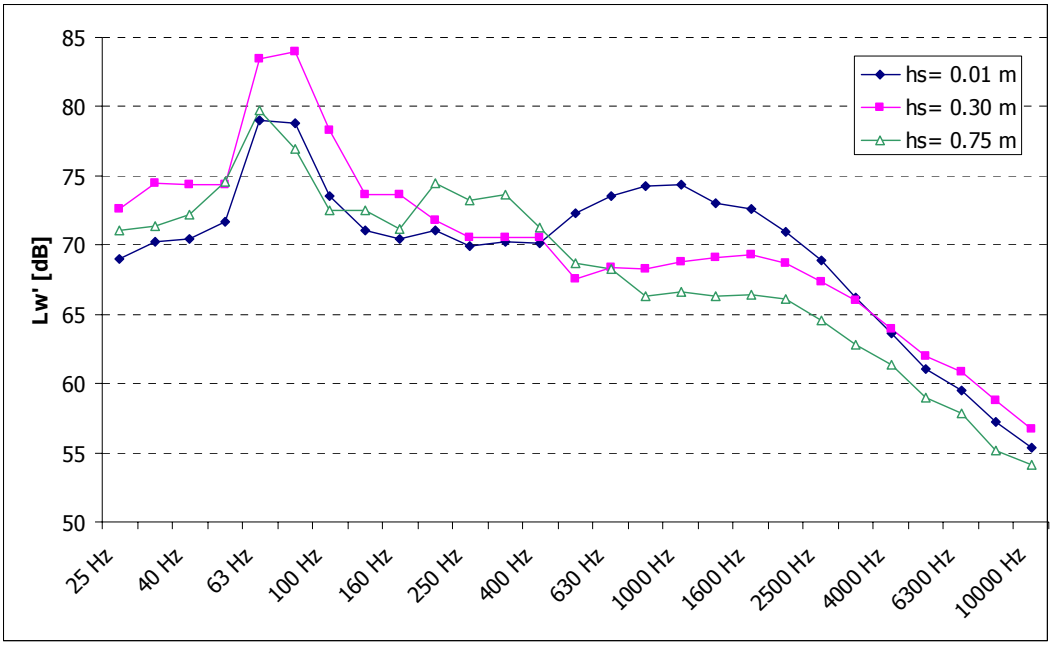

Buildings

All buildings have a rectangular lay-out and their shape is defined by flat roof surfaces. Facades are perfectly vertical and have an energy reflection coefficient, specified in the field "Fact_refl".

Meteorology

Sufficient meteorological variation will be achieved by combination of wind speed class W3, stability class S4 and wind direction class D6 according to [REF 3] (Southwest).

4 RESULTS

4.1 Case 01: Free field

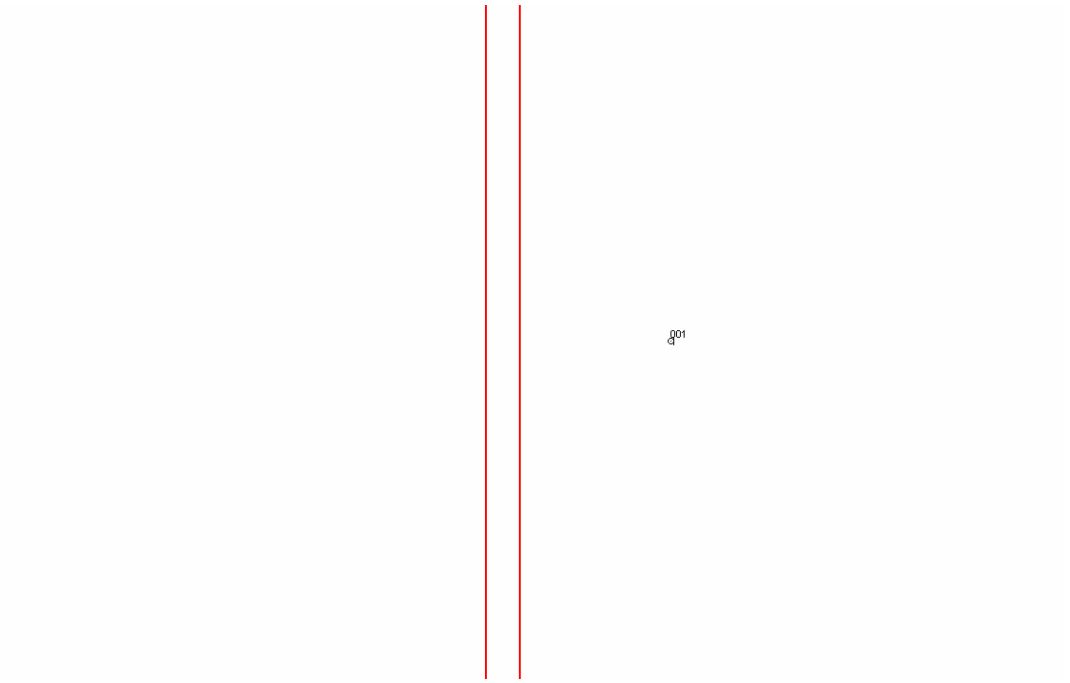

	Receiver	neutral	inversion	W3-S1 (SW)
map 01	001	68.5	69.3	68.4

In the following sections, the results of test maps 02 through 15 are compared graphically with the results of map 01 (except maps 09 and 10, since the position of receiver 001 has changed).

4.2 Case 02: Reflections

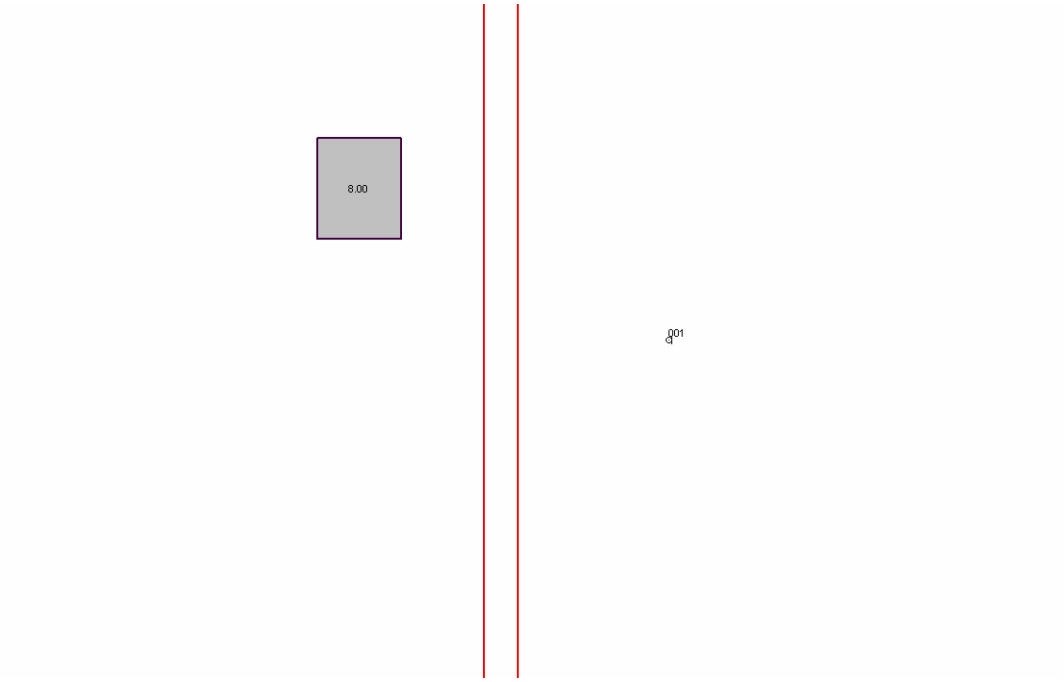

	Receiver	neutral	inversion	W3-S1 (SW)
map 02	001	68.7	69.5	68.5

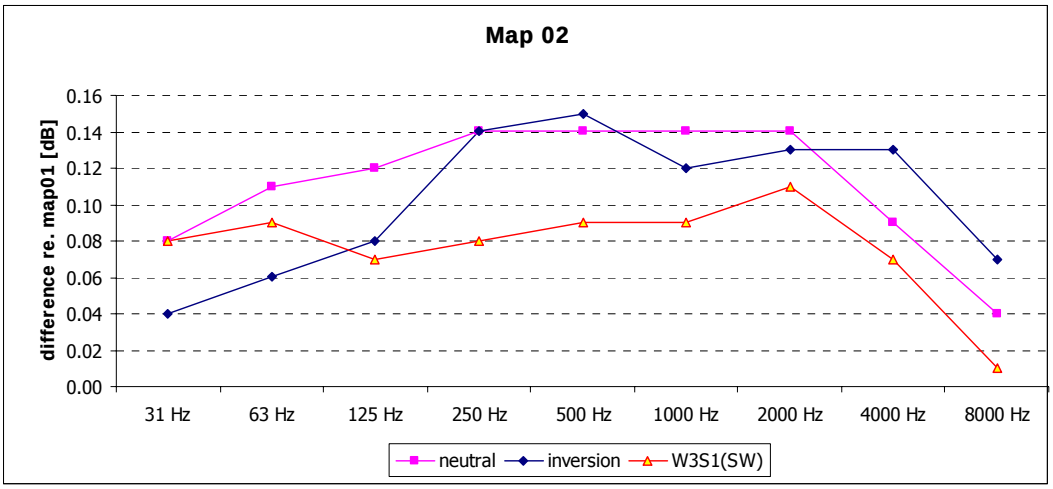

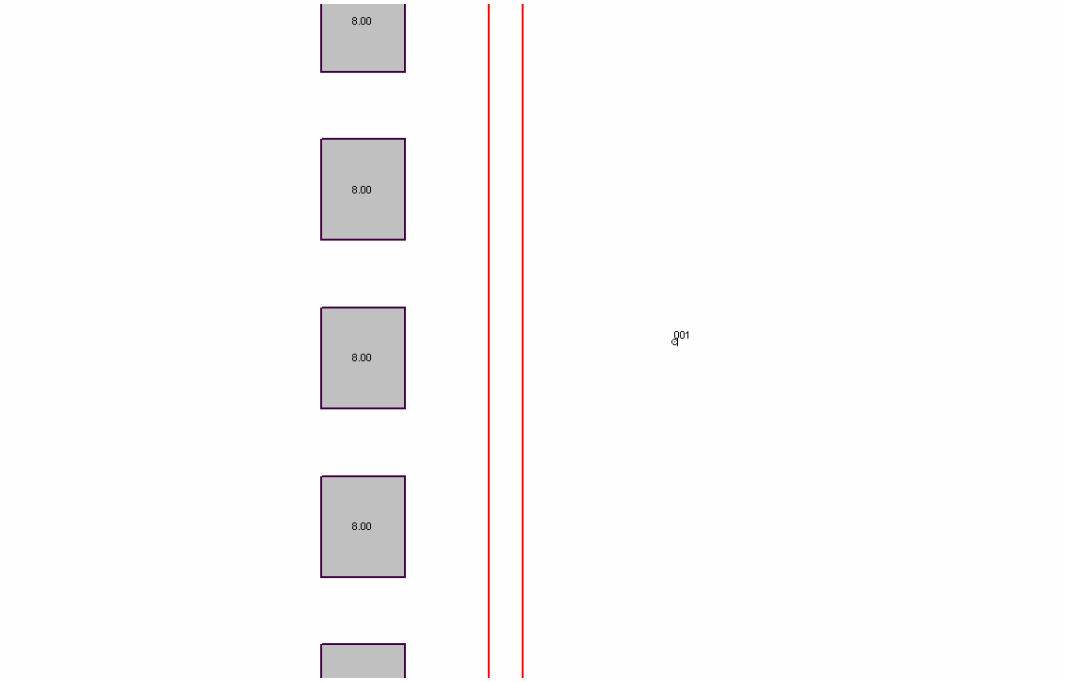

	Receiver	neutral	inversion	W3-S1 (SW)
map 03	001	69.2	69.8	68.9

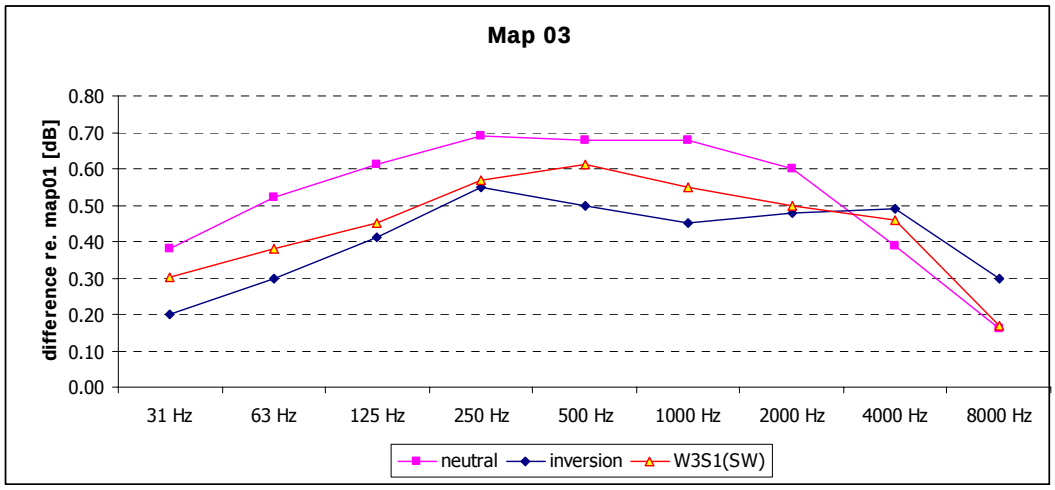

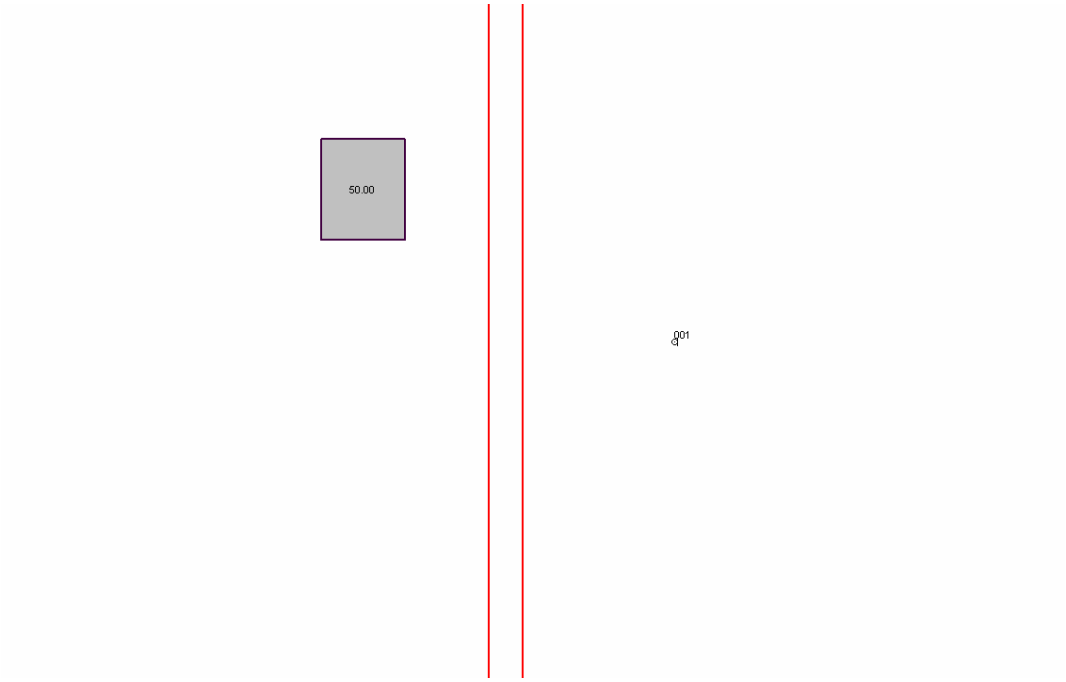

	Receiver	neutral	inversion	W3-S1 (SW)
map 04	001	68.7	69.5	68.5

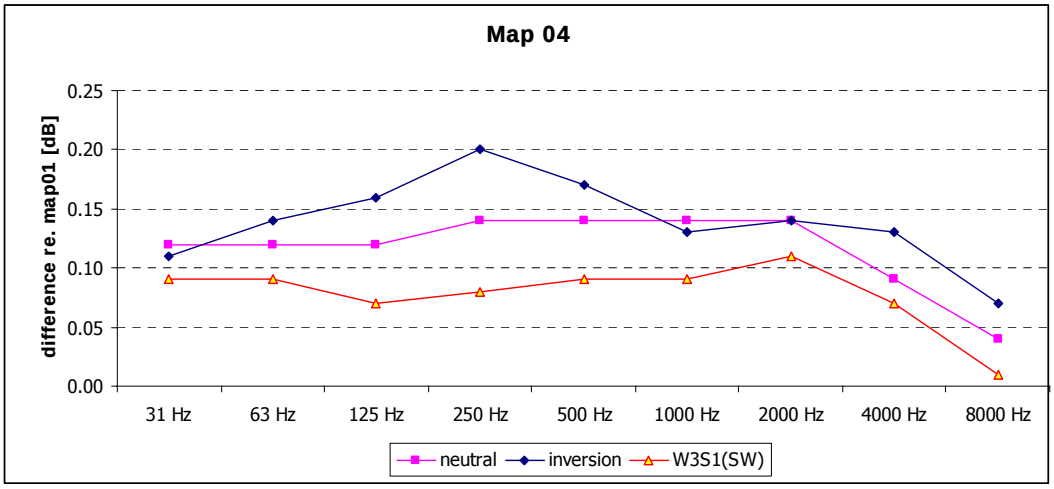

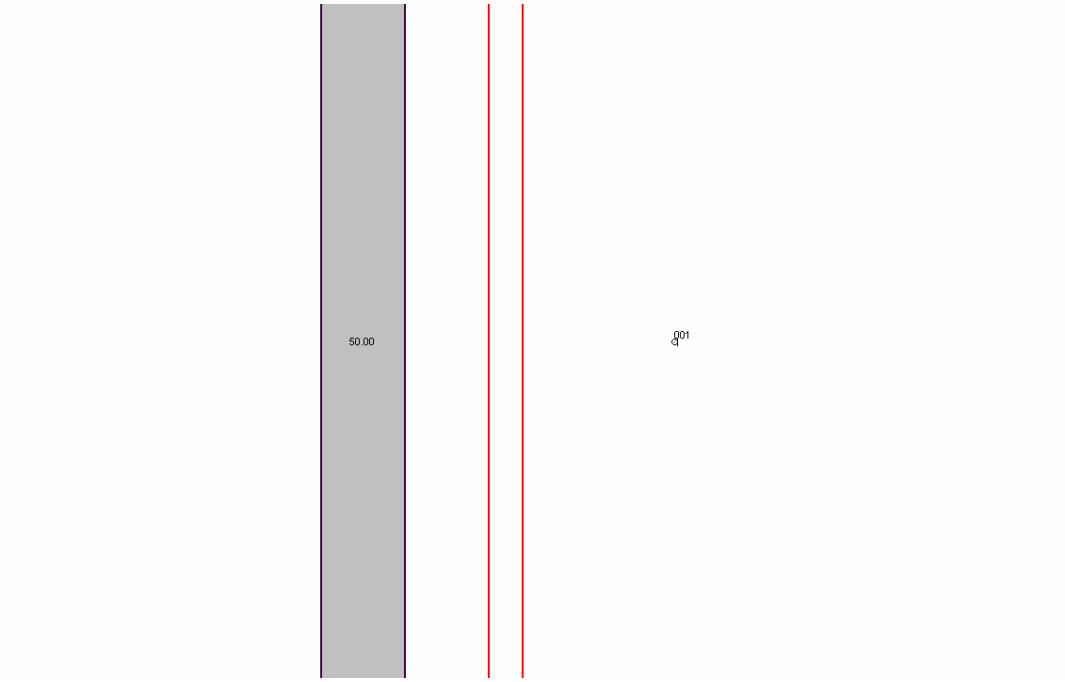

	Receiver	neutral	inversion	W3-S1 (SW)
map 05	001	69.6	69.6	68.8

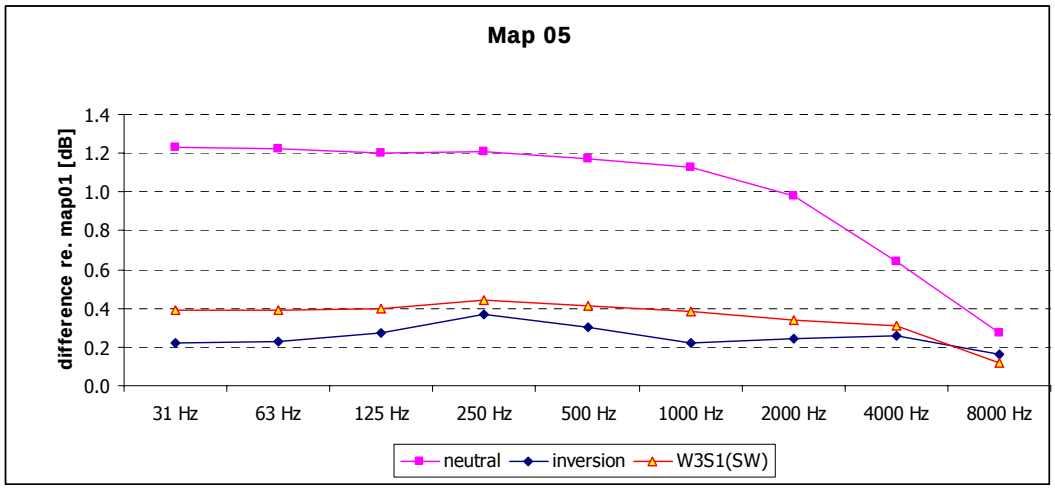

4.3 Case 03: Reflective plane behind the receiver

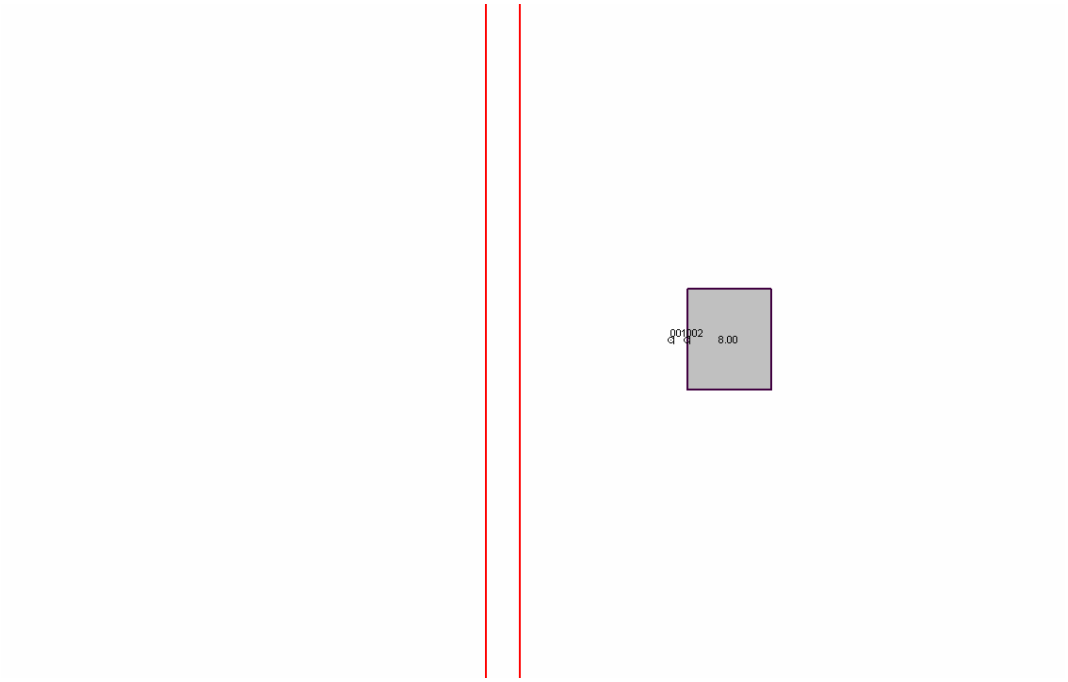

	Receiver	neutral	inversion	W3-S1 (SW)
map 06	001	70.5	71.2	70.4
	002	68.1	68.9	67.9

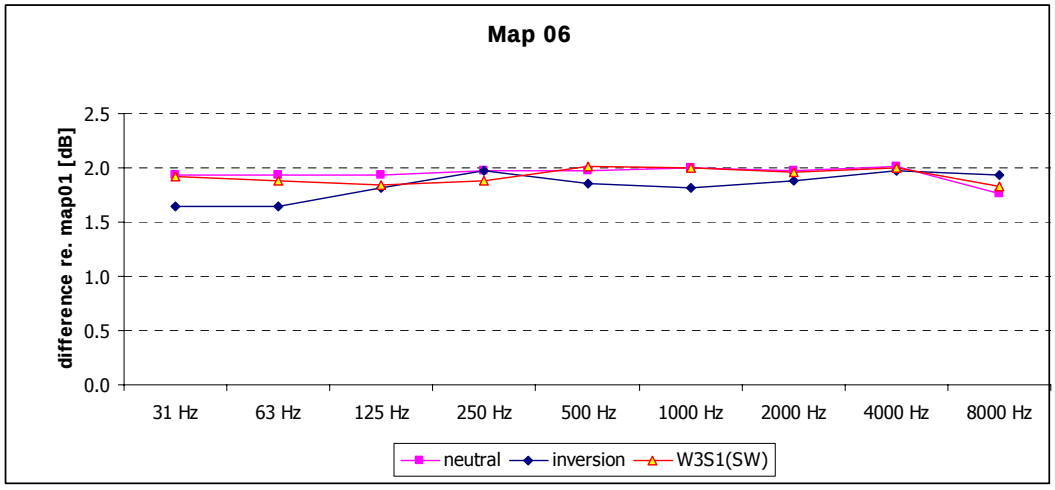

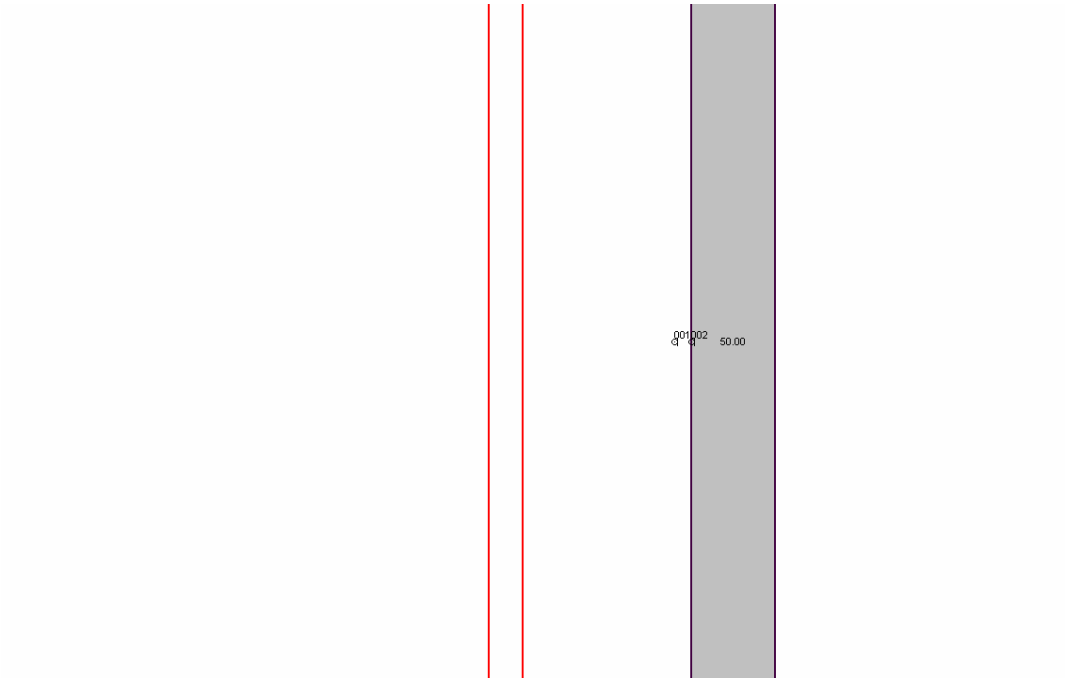

	Receiver	neutral	inversion	W3-S1 (SW)
map 07	001	70.7	69.7	68.9
	002	68.1	68.9	67.9

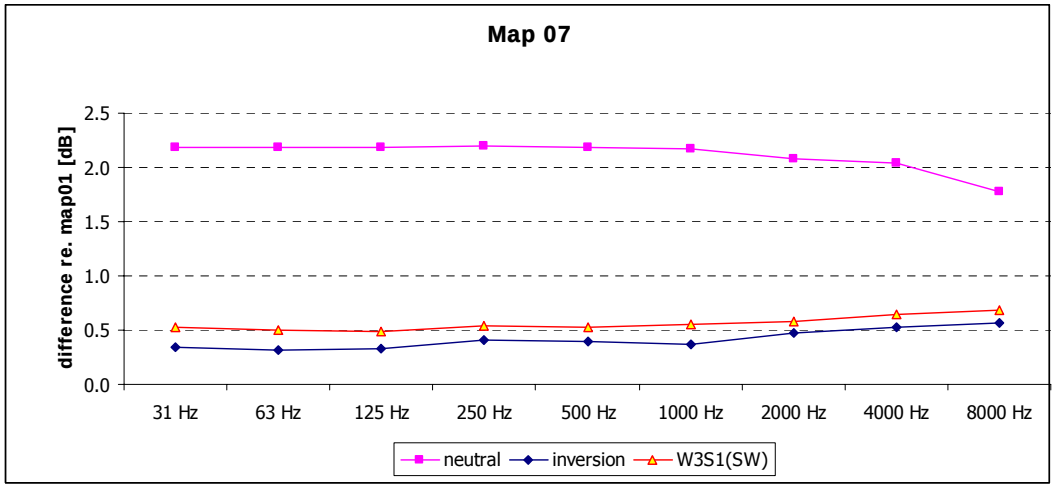

4.4 Case 04: Towards street canyons

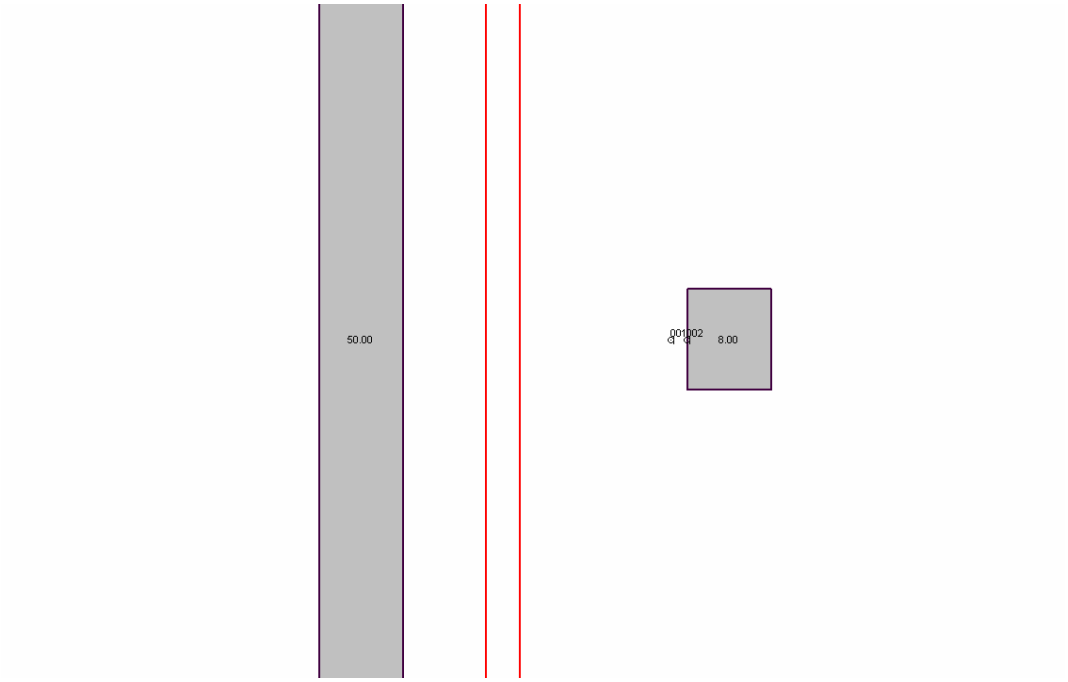

	Receiver	neutral	inversion	W3-S1 (SW)
map 08	001	71.9	71.6	70.9
	002	69.5	69.3	68.5

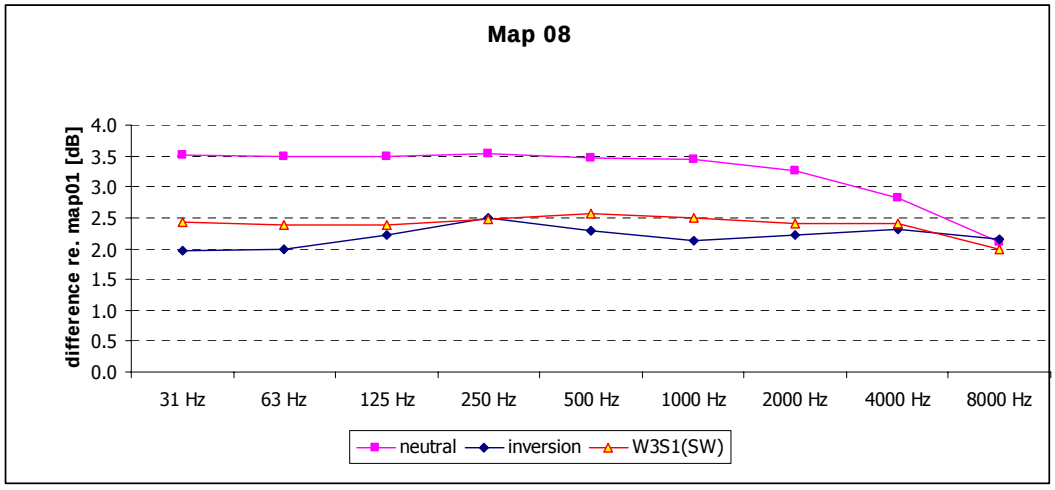

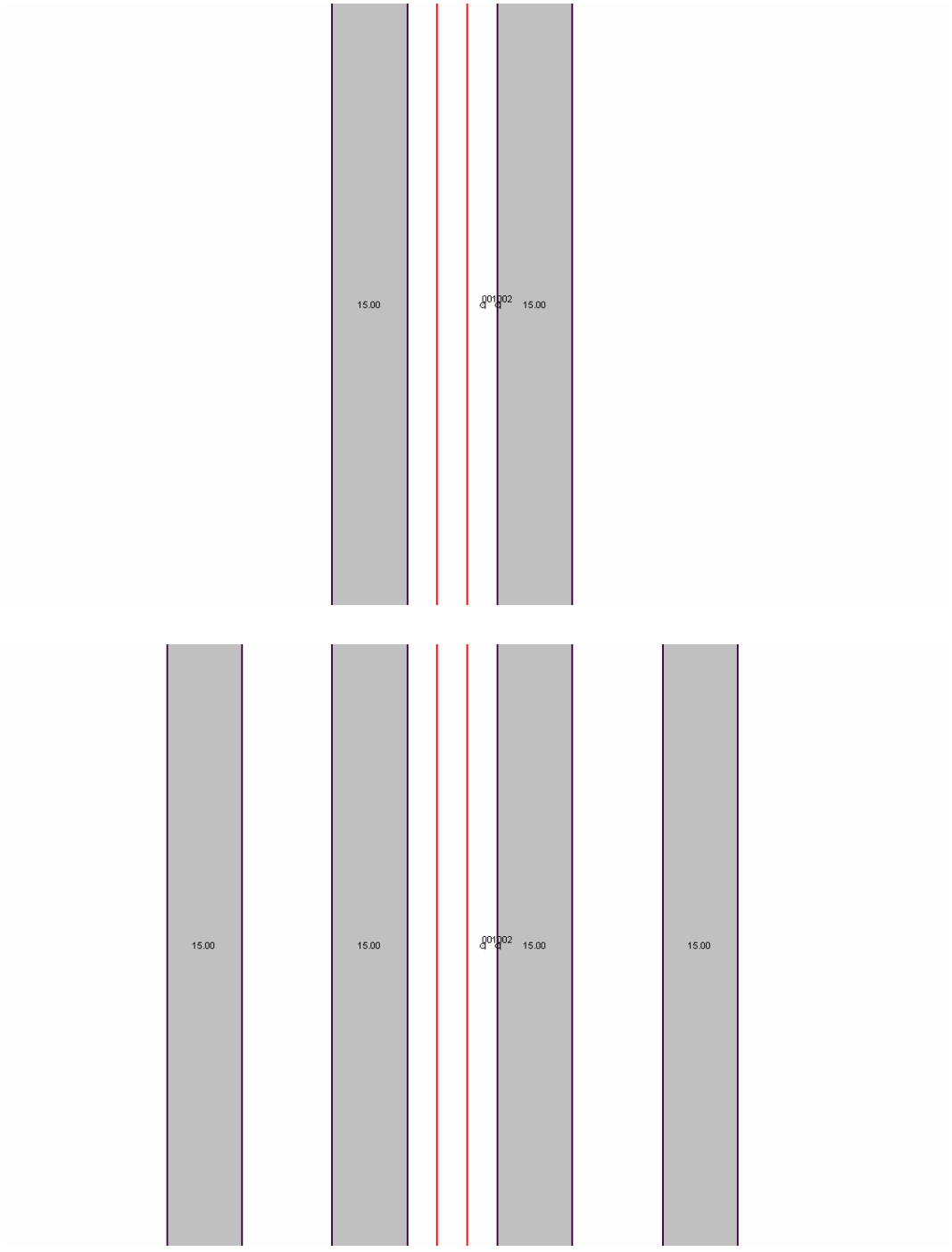

	Receiver	neutral	inversion	W3-S1 (SW)
map 09	001	78.8	76.5	76.3
	002	76.0	74.9	74.5
map 10	001	78.8	76.5	76.3
	002	76.0	74.9	74.5

4.5 Case 05: Screening by building blocks

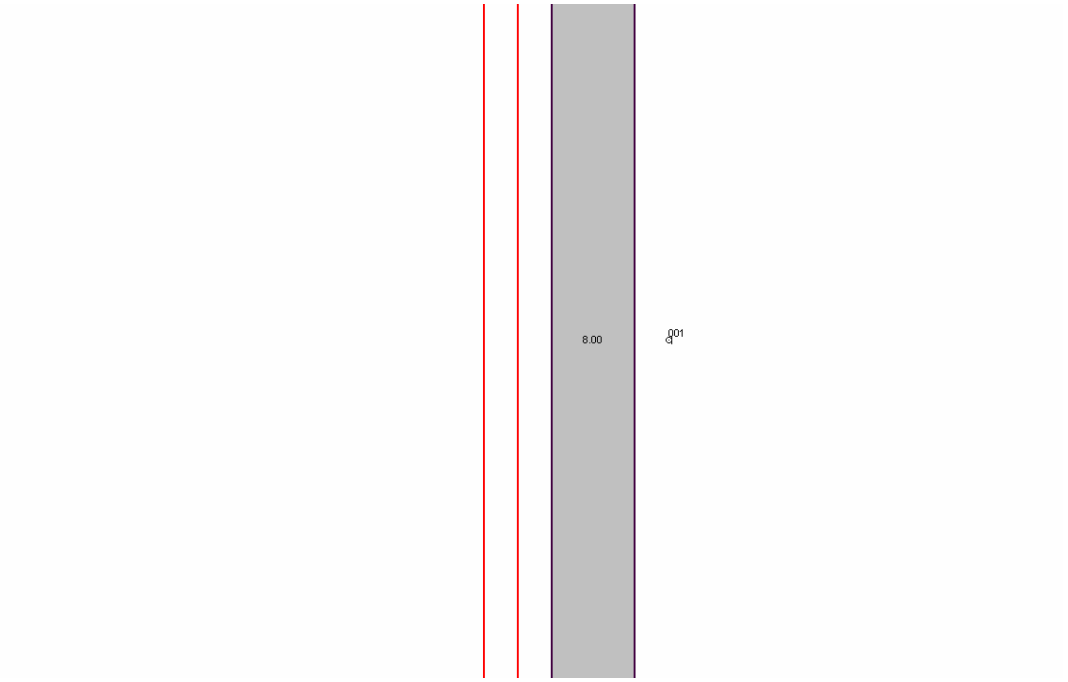

	Receiver	neutral	inversion	W3-S1 (SW)
map 11	001	40.7	55.9	43.0

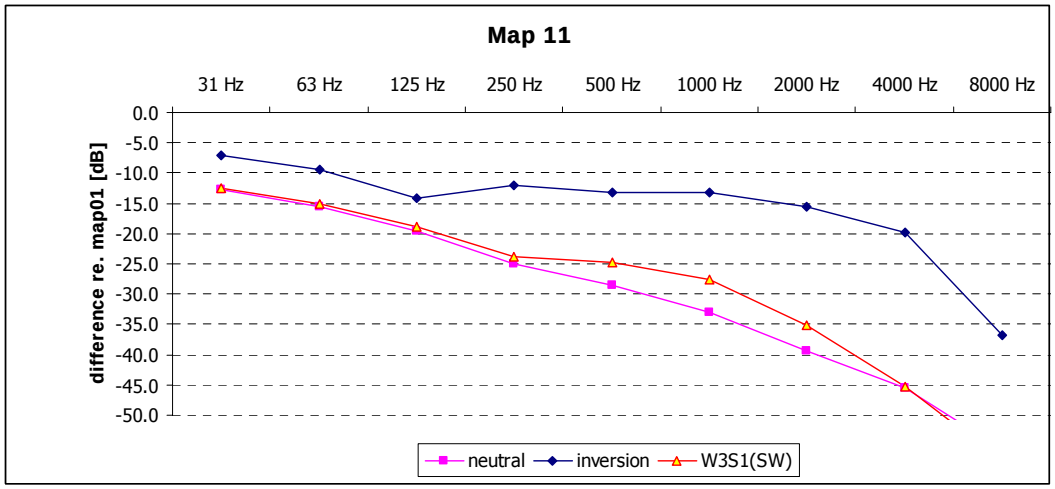

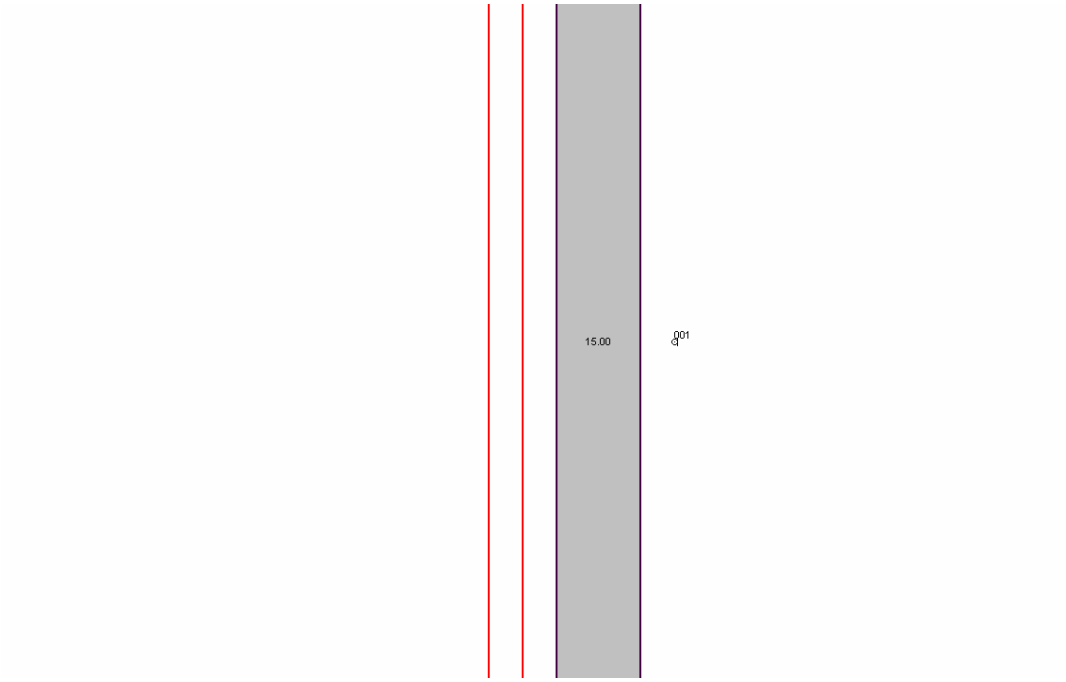

	Receiver	neutral	inversion	W3-S1 (SW)
map 12	001	30.7	50.9	31.8

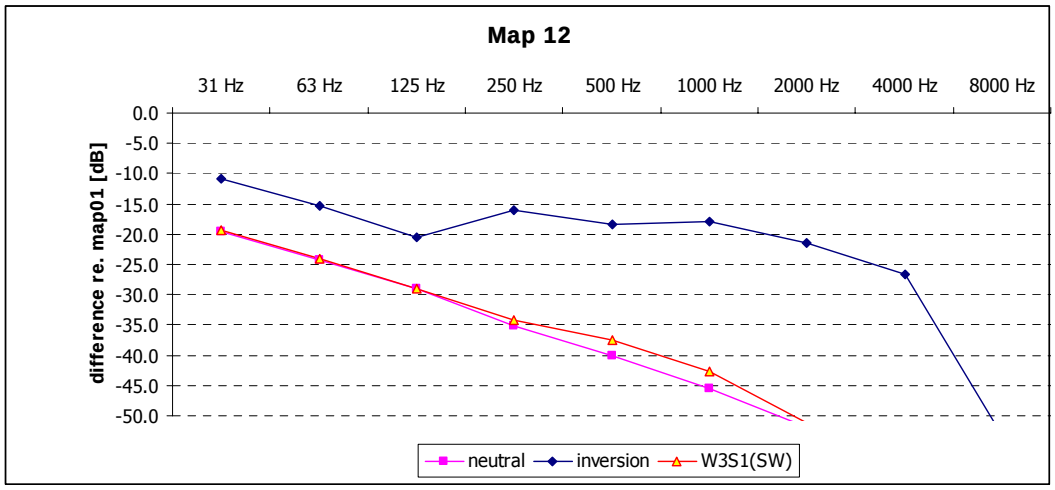

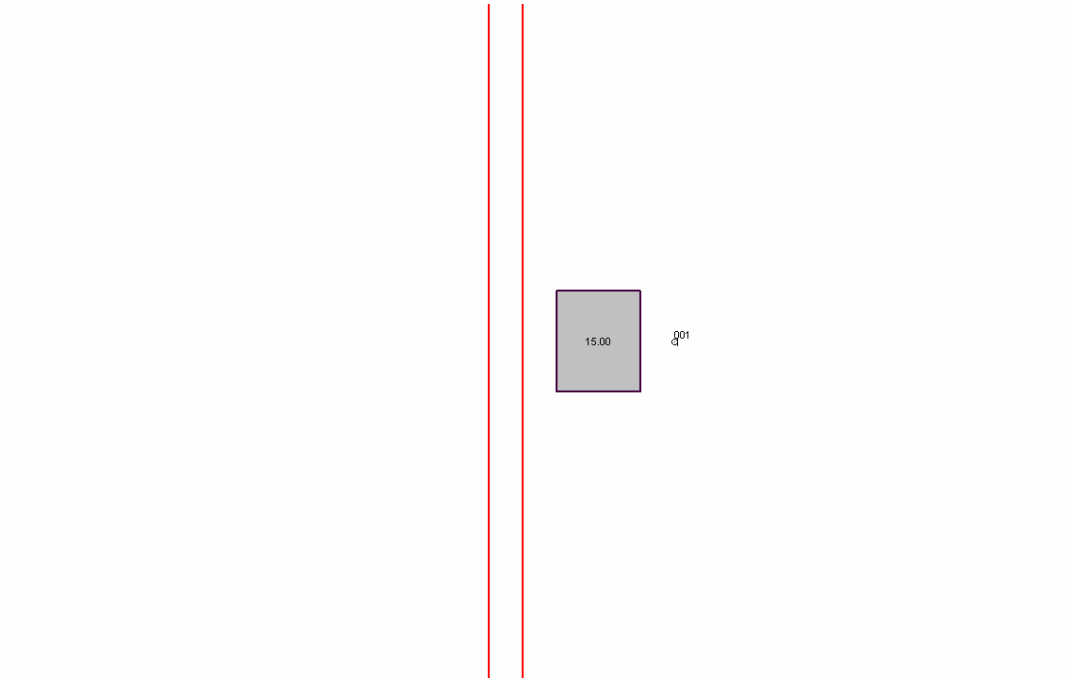

	Receiver	neutral	inversion	W3-S1 (SW)
map 13	001	62.9	65.0	62.7

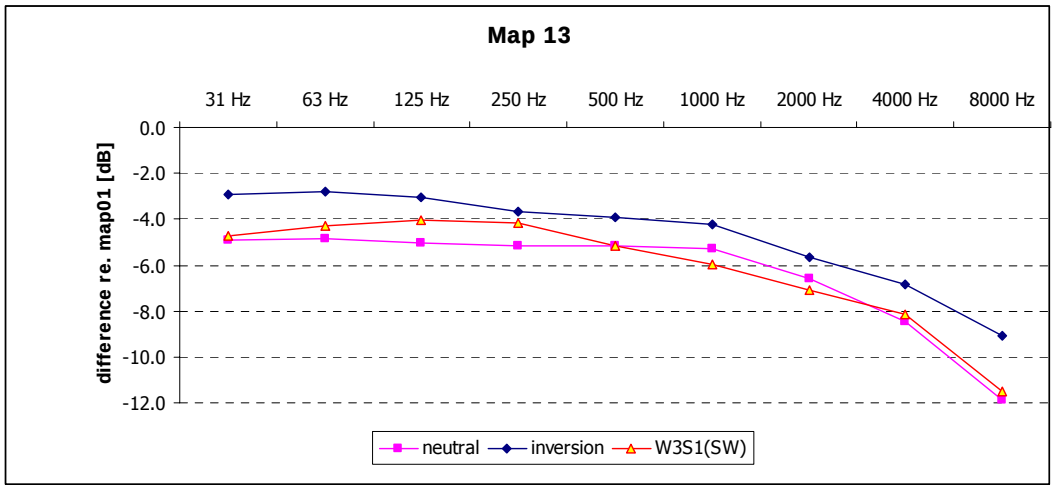

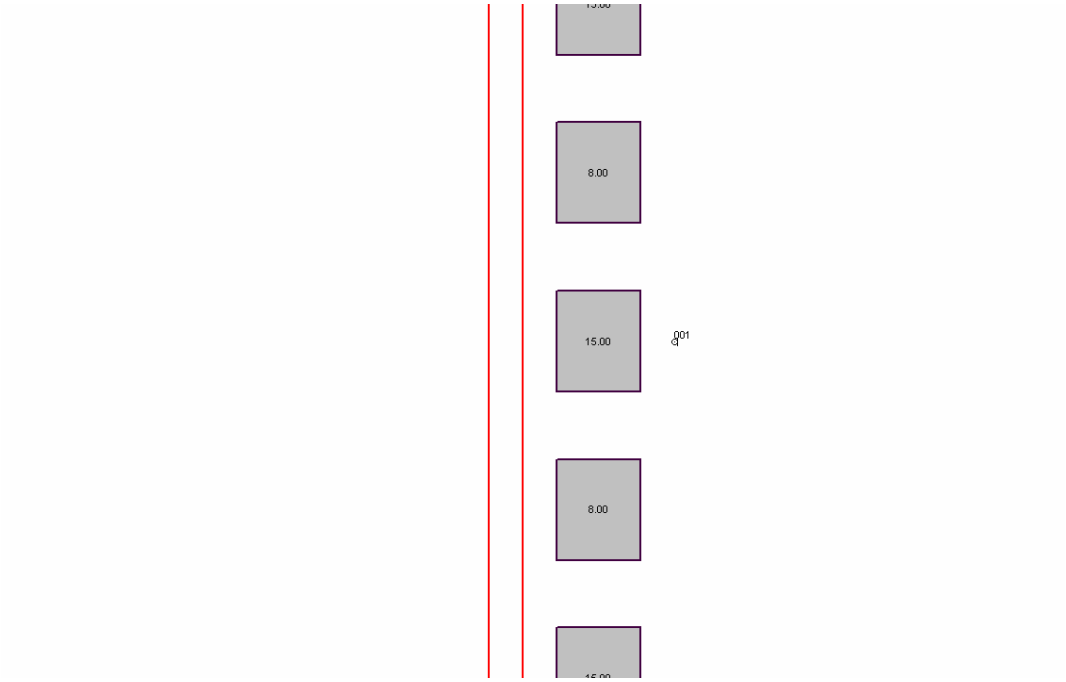

	Receiver	neutral	inversion	W3-S1 (SW)
map 14	001	49.4	54.3	49.7

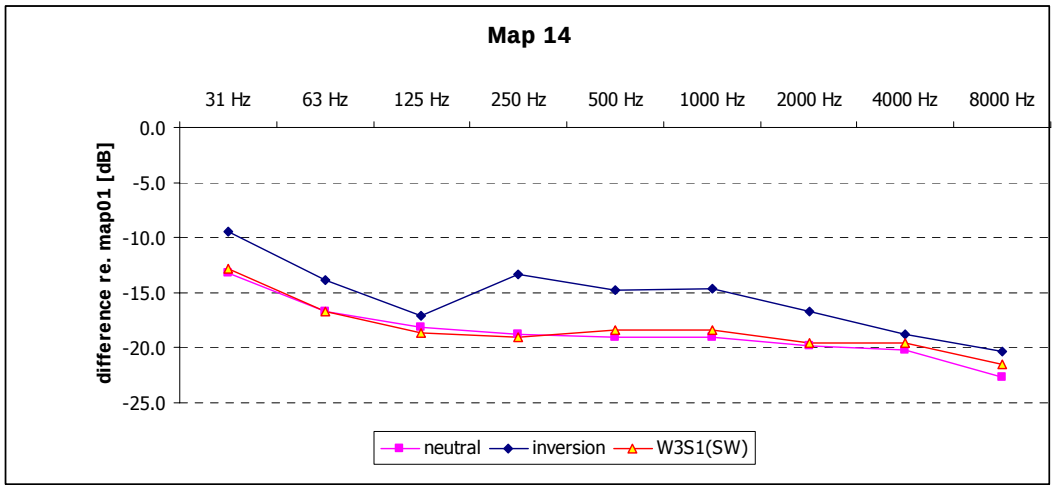

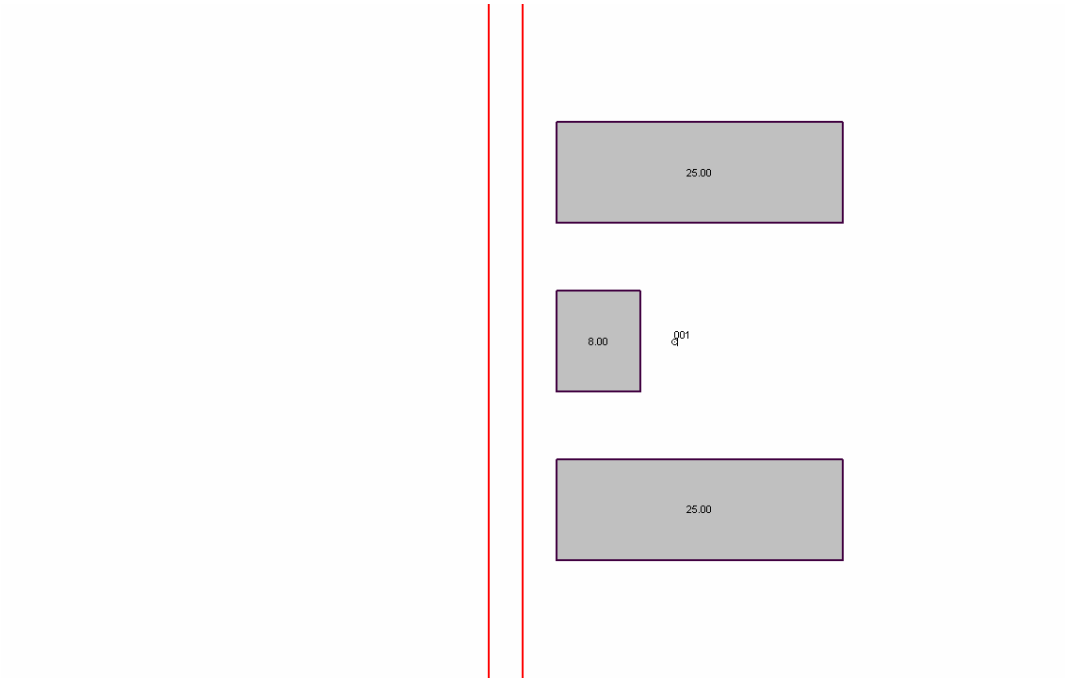

	Receiver	neutral	inversion	W3-S1 (SW)
map 15	001	56.7	57.5	56.4

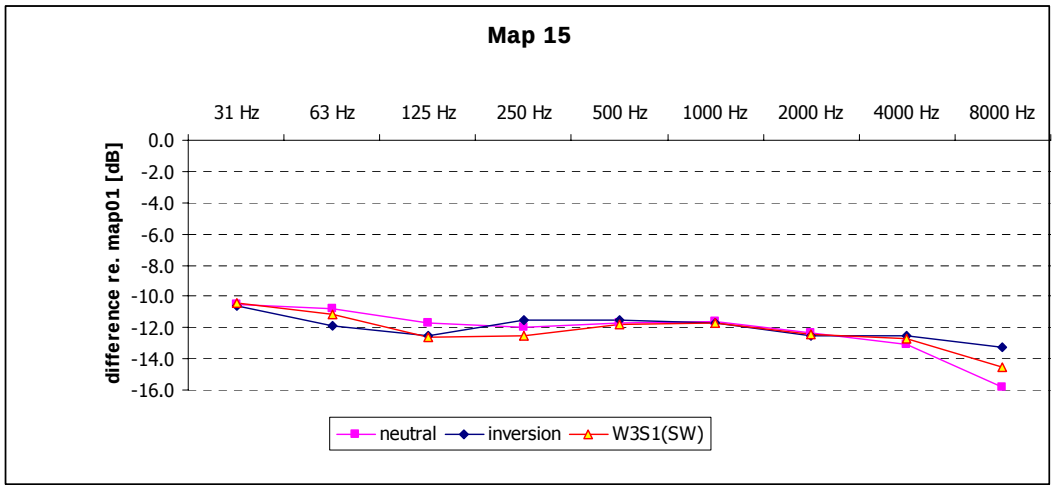

5 REFERENCES

REF 1 HAR70TR031126AEA01 "Mapping in urban situations",
REF 2 HAR32TR-040922-DGMR10 "Harmonoise WP 3 Engineering method for road traffic and railway noise after validation and fine-tuning".
REF 3 HAR25MO-031121-DLR01 "A unified meteorological classification".

Receivers

Id	X1	Y1	Z1	Type	Facade
1	1550.00	1000.00	4.00	free field	--

Roads

Id	X1	Y1	Z1	X2	Y2	Z2
1	1495.00	0.00	0.01	1495.00	2000.00	0.01
2	1495.00	0.00	0.30	1495.00	2000.00	0.30
3	1495.00	0.00	0.75	1495.00	2000.00	0.75
4	1505.00	0.00	0.01	1505.00	2000.00	0.01
5	1505.00	0.00	0.30	1505.00	2000.00	0.30
6	1505.00	0.00	0.75	1505.00	2000.00	0.75

Receivers

Id	X1	Y1	Z1	Type	Facade
1	1550.00	1000.00	4.00	free field	--

Roads

Id	X1	Y1	Z1	X2	Y2	Z2
1	1495.00	0.00	0.01	1495.00	2000.00	0.01
2	1495.00	0.00	0.30	1495.00	2000.00	0.30
3	1495.00	0.00	0.75	1495.00	2000.00	0.75
4	1505.00	0.00	0.01	1505.00	2000.00	0.01
5	1505.00	0.00	0.30	1505.00	2000.00	0.30
6	1505.00	0.00	0.75	1505.00	2000.00	0.75

Buildings

Id	X1	Y1	Z1	X2	Y2	Z2	X3	Y3	Z3	X4	Y4	Z4	Fact_refl
1	1470.00	1030.00	8.00	1470.00	1060.00	8.00	1445.00	1060.00	8.00	1445.00	1030.00	8.00	0.80

Receivers

Id	X1	Y1	Z1	Type	Facade
1	1550.00	1000.00	4.00	free field	--

Roads

Id	X1	Y1	Z1	X2	Y2	Z2
1	1495.00	0.00	0.01	1495.00	2000.00	0.01
2	1495.00	0.00	0.30	1495.00	2000.00	0.30
3	1495.00	0.00	0.75	1495.00	2000.00	0.75
4	1505.00	0.00	0.01	1505.00	2000.00	0.01
5	1505.00	0.00	0.30	1505.00	2000.00	0.30
6	1505.00	0.00	0.75	1505.00	2000.00	0.75

Buildings

Id	X1	Y1	Z1	X2	Y2	Z2	X3	Y3	Z3	X4	Y4	Z4	Fact_refl
1	1470.00	80.00	8.00	1470.00	110.00	8.00	1445.00	110.00	8.00	1445.00	80.00	8.00	0.80
2	1470.00	130.00	8.00	1470.00	160.00	8.00	1445.00	160.00	8.00	1445.00	130.00	8.00	0.80
3	1470.00	180.00	8.00	1470.00	210.00	8.00	1445.00	210.00	8.00	1445.00	180.00	8.00	0.80
4	1470.00	230.00	8.00	1470.00	260.00	8.00	1445.00	260.00	8.00	1445.00	230.00	8.00	0.80
5	1470.00	280.00	8.00	1470.00	310.00	8.00	1445.00	310.00	8.00	1445.00	280.00	8.00	0.80
6	1470.00	330.00	8.00	1470.00	360.00	8.00	1445.00	360.00	8.00	1445.00	330.00	8.00	0.80
7	1470.00	380.00	8.00	1470.00	410.00	8.00	1445.00	410.00	8.00	1445.00	380.00	8.00	0.80
8	1470.00	430.00	8.00	1470.00	460.00	8.00	1445.00	460.00	8.00	1445.00	430.00	8.00	0.80
9	1470.00	480.00	8.00	1470.00	510.00	8.00	1445.00	510.00	8.00	1445.00	480.00	8.00	0.80
10	1470.00	530.00	8.00	1470.00	560.00	8.00	1445.00	560.00	8.00	1445.00	530.00	8.00	0.80
11	1470.00	580.00	8.00	1470.00	610.00	8.00	1445.00	610.00	8.00	1445.00	580.00	8.00	0.80
12	1470.00	630.00	8.00	1470.00	660.00	8.00	1445.00	660.00	8.00	1445.00	630.00	8.00	0.80
13	1470.00	680.00	8.00	1470.00	710.00	8.00	1445.00	710.00	8.00	1445.00	680.00	8.00	0.80
14	1470.00	730.00	8.00	1470.00	760.00	8.00	1445.00	760.00	8.00	1445.00	730.00	8.00	0.80
15	1470.00	780.00	8.00	1470.00	810.00	8.00	1445.00	810.00	8.00	1445.00	780.00	8.00	0.80
16	1470.00	830.00	8.00	1470.00	860.00	8.00	1445.00	860.00	8.00	1445.00	830.00	8.00	0.80
17	1470.00	880.00	8.00	1470.00	910.00	8.00	1445.00	910.00	8.00	1445.00	880.00	8.00	0.80
18	1470.00	930.00	8.00	1470.00	960.00	8.00	1445.00	960.00	8.00	1445.00	930.00	8.00	0.80
19	1470.00	980.00	8.00	1470.00	1010.00	8.00	1445.00	1010.00	8.00	1445.00	980.00	8.00	0.80
20	1470.00	1030.00	8.00	1470.00	1060.00	8.00	1445.00	1060.00	8.00	1445.00	1030.00	8.00	0.80
21	1470.00	1080.00	8.00	1470.00	1110.00	8.00	1445.00	1110.00	8.00	1445.00	1080.00	8.00	0.80
22	1470.00	1130.00	8.00	1470.00	1160.00	8.00	1445.00	1160.00	8.00	1445.00	1130.00	8.00	0.80
23	1470.00	1180.00	8.00	1470.00	1210.00	8.00	1445.00	1210.00	8.00	1445.00	1180.00	8.00	0.80
24	1470.00	1230.00	8.00	1470.00	1260.00	8.00	1445.00	1260.00	8.00	1445.00	1230.00	8.00	0.80
25	1470.00	1280.00	8.00	1470.00	1310.00	8.00	1445.00	1310.00	8.00	1445.00	1280.00	8.00	0.80

Buildings

Id	X1	Y1	Z1	X2	Y2	Z2	X3	Y3	Z3	X4	Y4	Z4	Fact_refl
26	1470.00	1330.00	8.00	1470.00	1360.00	8.00	1445.00	1360.00	8.00	1445.00	1330.00	8.00	0.80
27	1470.00	1380.00	8.00	1470.00	1410.00	8.00	1445.00	1410.00	8.00	1445.00	1380.00	8.00	0.80
28	1470.00	1430.00	8.00	1470.00	1460.00	8.00	1445.00	1460.00	8.00	1445.00	1430.00	8.00	0.80
29	1470.00	1480.00	8.00	1470.00	1510.00	8.00	1445.00	1510.00	8.00	1445.00	1480.00	8.00	0.80
30	1470.00	1530.00	8.00	1470.00	1560.00	8.00	1445.00	1560.00	8.00	1445.00	1530.00	8.00	0.80
31	1470.00	1580.00	8.00	1470.00	1610.00	8.00	1445.00	1610.00	8.00	1445.00	1580.00	8.00	0.80
32	1470.00	1630.00	8.00	1470.00	1660.00	8.00	1445.00	1660.00	8.00	1445.00	1630.00	8.00	0.80
33	1470.00	1680.00	8.00	1470.00	1710.00	8.00	1445.00	1710.00	8.00	1445.00	1680.00	8.00	0.80
34	1470.00	1730.00	8.00	1470.00	1760.00	8.00	1445.00	1760.00	8.00	1445.00	1730.00	8.00	0.80
35	1470.00	1780.00	8.00	1470.00	1810.00	8.00	1445.00	1810.00	8.00	1445.00	1780.00	8.00	0.80
36	1470.00	1830.00	8.00	1470.00	1860.00	8.00	1445.00	1860.00	8.00	1445.00	1830.00	8.00	0.80
37	1470.00	1880.00	8.00	1470.00	1910.00	8.00	1445.00	1910.00	8.00	1445.00	1880.00	8.00	0.80
38	1470.00	1930.00	8.00	1470.00	1960.00	8.00	1445.00	1960.00	8.00	1445.00	1930.00	8.00	0.80
39	1470.00	1980.00	8.00	1470.00	2010.00	8.00	1445.00	2010.00	8.00	1445.00	1980.00	8.00	0.80

Receivers

Id	X1	Y1	Z1	Type	Facade
1	1550.00	1000.00	4.00	free field	--

Roads

Id	X1	Y1	Z1	X2	Y2	Z2
1	1495.00	0.00	0.01	1495.00	2000.00	0.01
2	1495.00	0.00	0.30	1495.00	2000.00	0.30
3	1495.00	0.00	0.75	1495.00	2000.00	0.75
4	1505.00	0.00	0.01	1505.00	2000.00	0.01
5	1505.00	0.00	0.30	1505.00	2000.00	0.30
6	1505.00	0.00	0.75	1505.00	2000.00	0.75

Buildings

Id	X1	Y1	Z1	X2	Y2	Z2	X3	Y3	Z3	X4	Y4	Z4	Fact_refl
1	1470.00	1030.00	50.00	1470.00	1060.00	50.00	1445.00	1060.00	50.00	1445.00	1030.00	50.00	0.80

Receivers

Id	X1	Y1	Z1	Type	Facade
1	1550.00	1000.00	4.00	free field	--

Roads

Id	X1	Y1	Z1	X2	Y2	Z2
1	1495.00	0.00	0.01	1495.00	2000.00	0.01
2	1495.00	0.00	0.30	1495.00	2000.00	0.30
3	1495.00	0.00	0.75	1495.00	2000.00	0.75
4	1505.00	0.00	0.01	1505.00	2000.00	0.01
5	1505.00	0.00	0.30	1505.00	2000.00	0.30
6	1505.00	0.00	0.75	1505.00	2000.00	0.75

Buildings

Id	X1	Y1	Z1	X2	Y2	Z2	X3	Y3	Z3	X4	Y4	Z4	Fact_refl
1	1470.00	0.00	50.00	1470.00	2000.00	50.00	1445.00	2000.00	50.00	1445.00	0.00	50.00	0.80

Receivers

Id	X1	Y1	Z1	Type	Facade
1	1550.00	1000.00	4.00	free field	--
2	1554.90	1000.00	4.00	facade	1

Roads

Id	X1	Y1	Z1	X2	Y2	Z2
1	1495.00	0.00	0.01	1495.00	2000.00	0.01
2	1495.00	0.00	0.30	1495.00	2000.00	0.30
3	1495.00	0.00	0.75	1495.00	2000.00	0.75
4	1505.00	0.00	0.01	1505.00	2000.00	0.01
5	1505.00	0.00	0.30	1505.00	2000.00	0.30
6	1505.00	0.00	0.75	1505.00	2000.00	0.75

Buildings

Id	X1	Y1	Z1	X2	Y2	Z2	X3	Y3	Z3	X4	Y4	Z4	Fact_refl
1	1580.00	985.00	8.00	1580.00	1015.00	8.00	1555.00	1015.00	8.00	1555.00	985.00	8.00	0.80

Receivers

Id	X1	Y1	Z1	Type	Facade
1	1550.00	1000.00	4.00	free field	--
2	1554.90	1000.00	4.00	facade	1

Roads

Id	X1	Y1	Z1	X2	Y2	Z2
1	1495.00	0.00	0.01	1495.00	2000.00	0.01
2	1495.00	0.00	0.30	1495.00	2000.00	0.30
3	1495.00	0.00	0.75	1495.00	2000.00	0.75
4	1505.00	0.00	0.01	1505.00	2000.00	0.01
5	1505.00	0.00	0.30	1505.00	2000.00	0.30
6	1505.00	0.00	0.75	1505.00	2000.00	0.75

Buildings

Id	X1	Y1	Z1	X2	Y2	Z2	X3	Y3	Z3	X4	Y4	Z4	Fact_refl
1	1580.00	0.00	50.00	1580.00	2000.00	50.00	1555.00	2000.00	50.00	1555.00	0.00	50.00	0.80

Receivers

Id	X1	Y1	Z1	Type	Facade
1	1550.00	1000.00	4.00	free field	--
2	1554.90	1000.00	4.00	facade	2

Roads

Id	X1	Y1	Z1	X2	Y2	Z2
1	1495.00	0.00	0.01	1495.00	2000.00	0.01
2	1495.00	0.00	0.30	1495.00	2000.00	0.30
3	1495.00	0.00	0.75	1495.00	2000.00	0.75
4	1505.00	0.00	0.01	1505.00	2000.00	0.01
5	1505.00	0.00	0.30	1505.00	2000.00	0.30
6	1505.00	0.00	0.75	1505.00	2000.00	0.75

Buildings

Id	X1	Y1	Z1	X2	Y2	Z2	X3	Y3	Z3	X4	Y4	Z4	Fact_refl
1	1470.00	0.00	50.00	1470.00	2000.00	50.00	1445.00	2000.00	50.00	1445.00	0.00	50.00	0.80
2	1580.00	985.00	8.00	1580.00	1015.00	8.00	1555.00	1015.00	8.00	1555.00	985.00	8.00	0.80

Receivers

Id	X1	Y1	Z1	Type	Facade
1	1510.00	1000.00	4.00	free field	--
2	1514.90	1000.00	4.00	facade	1

Roads

Id	X1	Y1	Z1	X2	Y2	Z2
1	1495.00	0.00	0.01	1495.00	2000.00	0.01
2	1495.00	0.00	0.30	1495.00	2000.00	0.30
3	1495.00	0.00	0.75	1495.00	2000.00	0.75
4	1505.00	0.00	0.01	1505.00	2000.00	0.01
5	1505.00	0.00	0.30	1505.00	2000.00	0.30
6	1505.00	0.00	0.75	1505.00	2000.00	0.75

Buildings

Id	X1	Y1	Z1	X2	Y2	Z2	X3	Y3	Z3	X4	Y4	Z4	Fact_refl
1	1540.00	0.00	15.00	1540.00	2000.00	15.00	1515.00	2000.00	15.00	1515.00	0.00	15.00	0.80
2	1485.00	0.00	15.00	1485.00	2000.00	15.00	1460.00	2000.00	15.00	1460.00	0.00	15.00	0.80

Receivers

Id	X1	Y1	Z1	Type	Facade
1	1510.00	1000.00	4.00	free field	--
2	1514.90	1000.00	4.00	facade	1

Roads

Id	X1	Y1	Z1	X2	Y2	Z2
1	1495.00	0.00	0.01	1495.00	2000.00	0.01
2	1495.00	0.00	0.30	1495.00	2000.00	0.30
3	1495.00	0.00	0.75	1495.00	2000.00	0.75
4	1505.00	0.00	0.01	1505.00	2000.00	0.01
5	1505.00	0.00	0.30	1505.00	2000.00	0.30
6	1505.00	0.00	0.75	1505.00	2000.00	0.75

Buildings

Id	X1	Y1	Z1	X2	Y2	Z2	X3	Y3	Z3	X4	Y4	Z4	Fact_refl
1	1540.00	0.00	15.00	1540.00	2000.00	15.00	1515.00	2000.00	15.00	1515.00	0.00	15.00	0.80
2	1485.00	0.00	15.00	1485.00	2000.00	15.00	1460.00	2000.00	15.00	1460.00	0.00	15.00	0.80
3	1430.00	0.00	15.00	1430.00	2000.00	15.00	1405.00	2000.00	15.00	1405.00	0.00	15.00	0.80
4	1595.00	0.00	15.00	1595.00	2000.00	15.00	1570.00	2000.00	15.00	1570.00	0.00	15.00	0.80

Receivers

Id	X1	Y1	Z1	Type	Facade
1	1550.00	1000.00	4.00	free field	--

Roads

Id	X1	Y1	Z1	X2	Y2	Z2
1	1495.00	0.00	0.01	1495.00	2000.00	0.01
2	1495.00	0.00	0.30	1495.00	2000.00	0.30
3	1495.00	0.00	0.75	1495.00	2000.00	0.75
4	1505.00	0.00	0.01	1505.00	2000.00	0.01
5	1505.00	0.00	0.30	1505.00	2000.00	0.30
6	1505.00	0.00	0.75	1505.00	2000.00	0.75

Buildings

Id	X1	Y1	Z1	X2	Y2	Z2	X3	Y3	Z3	X4	Y4	Z4	Fact_refl
1	1540.00	0.00	8.00	1540.00	2000.00	8.00	1515.00	2000.00	8.00	1515.00	0.00	8.00	0.80

Receivers

Id	X1	Y1	Z1	Type	Facade
1	1550.00	1000.00	4.00	free field	--

Roads

Id	X1	Y1	Z1	X2	Y2	Z2
1	1495.00	0.00	0.01	1495.00	2000.00	0.01
2	1495.00	0.00	0.30	1495.00	2000.00	0.30
3	1495.00	0.00	0.75	1495.00	2000.00	0.75
4	1505.00	0.00	0.01	1505.00	2000.00	0.01
5	1505.00	0.00	0.30	1505.00	2000.00	0.30
6	1505.00	0.00	0.75	1505.00	2000.00	0.75

Buildings

Id	X1	Y1	Z1	X2	Y2	Z2	X3	Y3	Z3	X4	Y4	Z4	Fact_refl
1	1540.00	0.00	15.00	1540.00	2000.00	15.00	1515.00	2000.00	15.00	1515.00	0.00	15.00	0.80

Receivers

Id	X1	Y1	Z1	Type	Facade
1	1550.00	1000.00	4.00	free field	--

Roads

Id	X1	Y1	Z1	X2	Y2	Z2
1	1495.00	0.00	0.01	1495.00	2000.00	0.01
2	1495.00	0.00	0.30	1495.00	2000.00	0.30
3	1495.00	0.00	0.75	1495.00	2000.00	0.75
4	1505.00	0.00	0.01	1505.00	2000.00	0.01
5	1505.00	0.00	0.30	1505.00	2000.00	0.30
6	1505.00	0.00	0.75	1505.00	2000.00	0.75

Buildings

Id	X1	Y1	Z1	X2	Y2	Z2	X3	Y3	Z3	X4	Y4	Z4	Fact_refl
1	1540.00	985.00	15.00	1540.00	1015.00	15.00	1515.00	1015.00	15.00	1515.00	985.00	15.00	0.80

Receivers

Id	X1	Y1	Z1	Type	Facade
1	1550.00	1000.00	4.00	free field	--

Roads

Id	X1	Y1	Z1	X2	Y2	Z2
1	1495.00	0.00	0.01	1495.00	2000.00	0.01
2	1495.00	0.00	0.30	1495.00	2000.00	0.30
3	1495.00	0.00	0.75	1495.00	2000.00	0.75
4	1505.00	0.00	0.01	1505.00	2000.00	0.01
5	1505.00	0.00	0.30	1505.00	2000.00	0.30
6	1505.00	0.00	0.75	1505.00	2000.00	0.75

Buildings

Id	X1	Y1	Z1	X2	Y2	Z2	X3	Y3	Z3	X4	Y4	Z4	Fact_refl
1	1540.00	985.00	15.00	1540.00	1015.00	15.00	1515.00	1015.00	15.00	1515.00	985.00	15.00	0.80
2	1540.00	685.00	15.00	1540.00	715.00	15.00	1515.00	715.00	15.00	1515.00	685.00	15.00	0.80
3	1540.00	735.00	8.00	1540.00	765.00	8.00	1515.00	765.00	8.00	1515.00	735.00	8.00	0.80
4	1540.00	785.00	15.00	1540.00	815.00	15.00	1515.00	815.00	15.00	1515.00	785.00	15.00	0.80
5	1540.00	835.00	8.00	1540.00	865.00	8.00	1515.00	865.00	8.00	1515.00	835.00	8.00	0.80
6	1540.00	885.00	15.00	1540.00	915.00	15.00	1515.00	915.00	15.00	1515.00	885.00	15.00	0.80
7	1540.00	935.00	8.00	1540.00	965.00	8.00	1515.00	965.00	8.00	1515.00	935.00	8.00	0.80
8	1540.00	1035.00	8.00	1540.00	1065.00	8.00	1515.00	1065.00	8.00	1515.00	1035.00	8.00	0.80
9	1540.00	1085.00	15.00	1540.00	1115.00	15.00	1515.00	1115.00	15.00	1515.00	1085.00	15.00	0.80
10	1540.00	1135.00	8.00	1540.00	1165.00	8.00	1515.00	1165.00	8.00	1515.00	1135.00	8.00	0.80
11	1540.00	1185.00	15.00	1540.00	1215.00	15.00	1515.00	1215.00	15.00	1515.00	1185.00	15.00	0.80
12	1540.00	1235.00	8.00	1540.00	1265.00	8.00	1515.00	1265.00	8.00	1515.00	1235.00	8.00	0.80
13	1540.00	1285.00	15.00	1540.00	1315.00	15.00	1515.00	1315.00	15.00	1515.00	1285.00	15.00	0.80

Receivers

Id	X1	Y1	Z1	Type	Facade
1	1550.00	1000.00	4.00	free field	--

Roads

Id	X1	Y1	Z1	X2	Y2	Z2
1	1495.00	0.00	0.01	1495.00	2000.00	0.01
2	1495.00	0.00	0.30	1495.00	2000.00	0.30
3	1495.00	0.00	0.75	1495.00	2000.00	0.75
4	1505.00	0.00	0.01	1505.00	2000.00	0.01
5	1505.00	0.00	0.30	1505.00	2000.00	0.30
6	1505.00	0.00	0.75	1505.00	2000.00	0.75

Buildings

Id	X1	Y1	Z1	X2	Y2	Z2	X3	Y3	Z3	X4	Y4	Z4	Fact_refl
1	1540.00	985.00	8.00	1540.00	1015.00	8.00	1515.00	1015.00	8.00	1515.00	985.00	8.00	0.80
2	1600.00	1035.00	25.00	1600.00	1065.00	25.00	1515.00	1065.00	25.00	1515.00	1035.00	25.00	0.80
3	1600.00	935.00	25.00	1600.00	965.00	25.00	1515.00	965.00	25.00	1515.00	935.00	25.00	0.80